FINAL TECHNICAL REPORT

POWER CYLINDER FRICTION REDUCTION THROUGH COATINGS, SURFACE FINISH AND DESIGN

U.S. Department of Energy Award DE-EE0006901

January 1, 2015 – March 31, 2021

Submitted By:

Arup Gangopadhyay
Principal Investigator
Ford Motor Company

Partner Organizations:

Argonne National Laboratories

June 2021

ACKNOWLEDGMENTS

This material is based on work partially funded by the U.S. Department of Energy National Technology Laboratory through Cooperative Agreement DE-EE0006901.

The author acknowledges the assistance and support of the following individuals for their expertise and participation in this project as well as their collaboration and effort in writing this final report.

Ford Motor Company: A. Gangopadhyay, R.J. Zdrodowski, Zak Liu, Larry Elie, Cliff Maki, Joachim Patschull

Argonne National Laboratory: A. Erdemir, G. Ramirez, Levent Eryilmaz

Table of Contents

EXECUTIVE SUMMARY

About 7-10% of the total energy input in a vehicle is lost due to mechanical friction, and in an engine, about 50% of the total frictional losses occur at the interface between the cylinder and pistons and piston rings. Therefore, this interface offers great opportunities for friction reduction. The goal of this proposed study is to demonstrate friction reduction potential using advanced coatings, surface finish, and design on power cylinder system containing cylinder bore, piston rings, crankshaft, and advanced engine oils. Experience through years of research in this area lead us to believe that full benefit potential can be realized only by considering a systems approach.

This investigation explored friction reduction opportunities through a bundle of technologies including thermal spray coating on cylinder bore, several piston ring face coatings, improved surface finish on cylinder bore and crankshaft journals, and low friction polyalkylene glycol engine oil. Thermal spray coatings are increasingly being introduced in high volume engines by different engine manufacturers including Ford. These are thick coatings (about 150 micrometer) and deposited by various techniques i.e., plasma transfer wire arc (PTWA), electric wire arc, twin wire arc etc. These coatings contain low porosity (<2%) and extensive prior research in our laboratory did not show a friction benefit from PTWA coating over cast iron liner material. One of the goals of this project is to explore development of high porosity PTWA coatings with the aim to reduce frictional losses. The porosity levels were divided into four categories; <2%, 3-5%, 6-8% and >8%. Micro-polishing of crank journal was pursued as another friction reduction opportunity. Other technologies investigated include ring coatings (Mo-NiCr, PVD (physical vapor deposition), DLC diamond-like carbon), and Nitride), and PAG (polyalkylene glycol) oil, obtained from suppliers.

Friction assessments were conducted at different levels, starting from laboratory bench test rigs to in-house developed component level tests including engine cranktrain only (included friction contributions from piston, piston rings, cylinder bore surface, and bearings), motored unpressurized single cylinder engine, which measured friction at piston and cylinder bore interface followed by full engine motored friction tests. Friction benefit under engine firing conditions was captured through fired single cylinder engine and chassis roll fuel economy tests.

High porosity PTWA coating development was pursued with Comau and honing development with Gehring. Initial coating development was focused on small flat coupons to understand various factors affecting porosity levels and then identified the critical control factors and their levels. The critical factors identified were atomizing gas pressure, wire feed rate, plasma gas flow rate, current, and nozzle (plasma torch) design. However, when these factors were applied for coating deposition on free-standing liners, the porosity levels on liner surface turned out to be much lower than expected. This is due to closing of pores by the honing process. Therefore, an extensive study was conducted to tune honing conditions to keep the pores open and also to generate additional pores enabling creation of porosity levels much higher than the target levels. The honing process also created a mirror finish on the bore.

Laboratory bench friction tests conducted with a section of these liners and a section of current production piston rings showed significant friction benefit in mixed lubrication regime over cast iron liner and the benefit increased with increasing porosity levels. In addition, selection of ring face coating, particularly diamond-like carbon coating (DLC) in contact with high porosity PTWA coating showed additional friction benefit over cast iron both in boundary and mixed lubrication regimes. Cranktrain tests where friction contributions included from piston ring and cylinder bore surface showed similar results as the laboratory bench tests. The friction benefit increased with increasing oil temperature. The friction benefit with various ring face coatings depended on crankshaft speed and temperature. More benefits

were observed at higher speeds. The motored unpressurized single cylinder engine friction tests showed similar results. The same cranktrain friction rig was used for evaluation of friction reduction potential of micro-polished crank journals (both rods and mains). The results showed little friction benefit over production finish at higher crankshaft speed. The expectation was that benefit would be seen more on lower speeds under mixed lubrication regime. It is possible that the benefit at higher speeds may be due to increased bearing clearance from polishing.

Several liner-less engine blocks were made with high porosity PTWA coatings and engines were built with those blocks. The engines were broken-in for one hundred hours in a dyno followed by motoring until a stable friction response was observed at each engine speeds. The tests were conducted at four oil temperatures, 35/40^{o}C, 60^{o}C, 90^{o}C, and 120^{o}C. At each temperature significant friction benefit was observed over the production engine with cast iron liner. An average (over the speed range investigated) friction benefit of 5% was observed with a block with the highest porosity level. In general, the friction benefit correlated with porosity level; higher the porosity, higher the friction reduction.

Fired single cylinder friction tests were conducted on twelve load-speed points using a Ricardo Hydra engine. The results indicated in general lower friction with PTWA coated liner than uncoated cast iron liner. However, high load and high speed points led to scuffing and wear on piston skirt and liner surfaces. This engine did not use any (skirt) coated piston and that is suspected to cause scuffing and wear.

The engine that showed the highest friction benefit in motored engine friction tests was used for chassis roll fuel economy tests. However, a few components were changed. The production crankshaft was replaced with a crankshaft with micro-polished journals, the top and oil control rings were replaced with DLC coated rings in order to show the fuel economy benefit of the technology bundle. The results showed a fuel economy benefit of 0.8% and 4.7% in metro-highway cycles with GF-5 SAE 5W-20 and PAG oil 15-1 oils respectively. Although PAG oil showed a high fuel economy benefit, prior investigation (DE-EE0005388) revealed issues with wear protection and varnish formation.

The wear characteristics of high porosity PTWA coating and piston (oil control) rings were evaluated using a radio tracer technique on a motored cranktrain rig and compared with a production engine block with cast iron liner. The results indicated that the wear rate of high porosity PTWA coating is comparable to cast iron liner with current production rings and with PVD rings. The wear rate of current production ring wear was higher with high porosity PTWA coating than cast iron liner. But the wear rate of DLC coated rings was lower than production nitrided rings with both high porosity PTWA and cast iron liner. In addition, lower friction was observed.

In summary, the project (a) identified a detailed process for deposition and honing of PTWA coatings at various porosity levels, (b) identified porosity level for highest friction reduction and fuel economy improvement, (c) identified ring coating for additional friction benefit, and (d) demonstrated durability of high porosity PTWA coating and identified a ring coating for reduced friction while maintaining durability.

1.0 INTRODUCTION

About 7-10% of the total energy input in a vehicle is lost due to mechanical friction (1), and therefore offers great opportunities for friction reduction. In an engine, about 60% of the total frictional losses occur at the interface between the cylinder and pistons and piston rings, and about 30% at the bearings as shown in Figure 1 (2). The goal of this proposed study is to demonstrate friction reduction potential using advanced coatings, surface finish, and design on power cylinder system containing cylinder bore, piston rings, crankshaft, and advanced engine oils. Experience through years of research in this area lead us to believe that full benefit potential can be realized only by considering a systems approach.

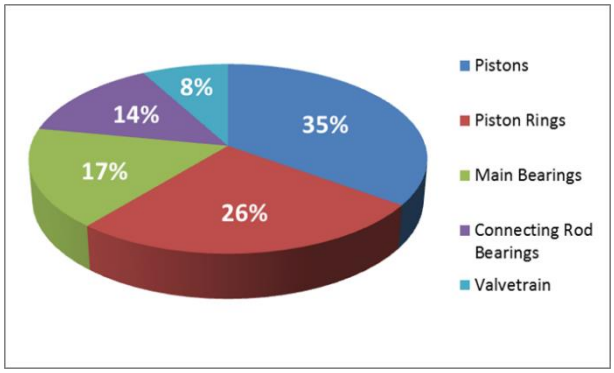

Figure 1. The distribution of frictional losses in an engine.

It is important to understand the lubrication regimes under which the piston ring and cylinder bore contact operate. Figure 2 shows the distribution of minimum oil film thickness during the four strokes of a gasoline engine at two different speeds. The oil film thickness is highest at the middle of the stroke and at higher speeds as expected. Also, the oil film thickness is lower during power stroke because of the high gas pressure. The oil film thickness at the second compression ring is lower than the top compression ring during the power stroke. The surface roughness (Rq) of typical cylinder bore and piston ring surfaces are 0.50 μm and 0.3 μm respectively, which lend a composite surface roughness of 0.6 μm. Two lines are drawn on each figure at film thicknesses which correspond to specific film thickness of 1 and 3, thus separating boundary, mixed and hydrodynamic lubrication regimes. It can be observed that the top compression ring (1st ring) operates under boundary and mixed lubrication regimes at 1000 RPM even at the middle of the stroke. But at 4000 RPM, the top compression ring operates under hydrodynamic regime for a significant part of the stroke. The second ring operates similarly. Therefore, depending on the engine speed and oil temperature the rings may operate under boundary and mixed lubrication regimes indicating the importance of asperity interactions at this contact. The surface asperity interactions can be controlled by improved surface finish and deposition of low friction coatings.

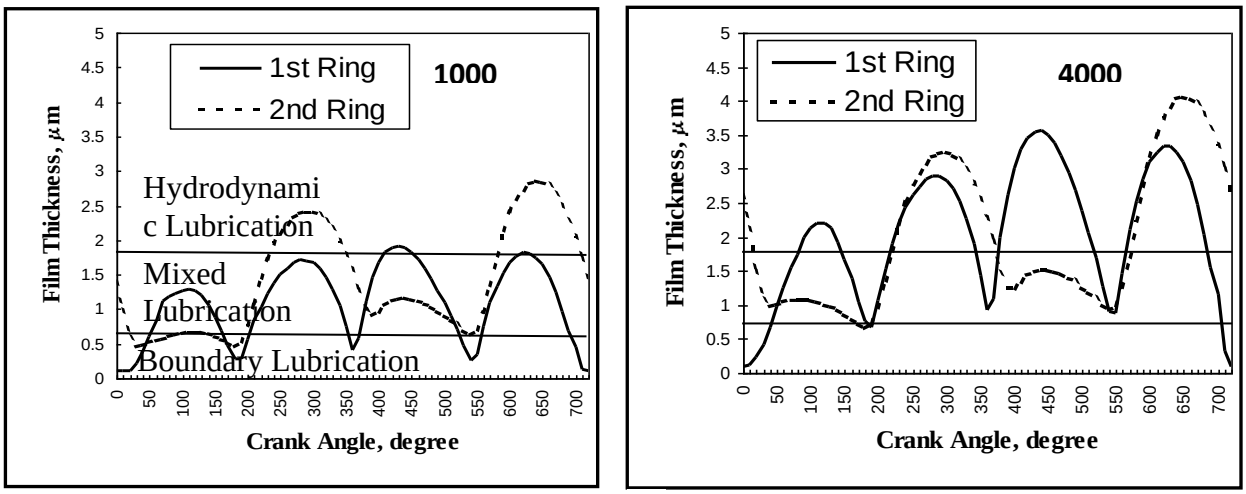

(a) (b)

Figure 2. Minimum oil film distribution at the piston ring cylinder interface at (a) 1000 RPM, and (b) 4000 RPM.

The research focused on opportunities on cylinder bore, piston ring, and crankshaft surface finish in engine power cylinder system.

Cylinder bore surface - Deposition of coatings on cylinder surface has been studied over twenty five years. Most of these investigations were focused on aluminum blocks to replace cast iron liners for potential weight saving with improved fuel economy. Nickel composite coatings (deposited by electrochemical technique) were developed for automotive and marine engines in early nineties to address corrosion issues related to use of methanol (M85) fuels (3,4). Solid lubricant based coatings (deposited by plasma spray technique) were developed by Ford in late nineties to improve wear resistance and friction reduction (5). Recently, plasma transferred wire arc (PTWA) coatings gained a lot of attention and its use in engines significantly grew from limited volume vehicles (6,7) to high volume vehicles. Figure 3 shows the industry landscape on adoption of thermal spray technologies for cylinder bore surface. This includes Twin Wire Arc Process, and Electric Wire Arc process. These thermal spray processes contain low porosity (less than 2%) and not necessarily reduce friction. The PTWA process is a thermal spray process and suitable for depositing coatings on both cast iron and aluminum surfaces. The deposition rate achieved by this process is much higher than that achieved with conventional plasma spray process and also at a lower power level. The lower heat input to the deposited coating leads to reduced residual stress allowing deposition of thick coatings. The objective of this investigation is to develop high porosity PTWA coatings enabling significant friction reduction.

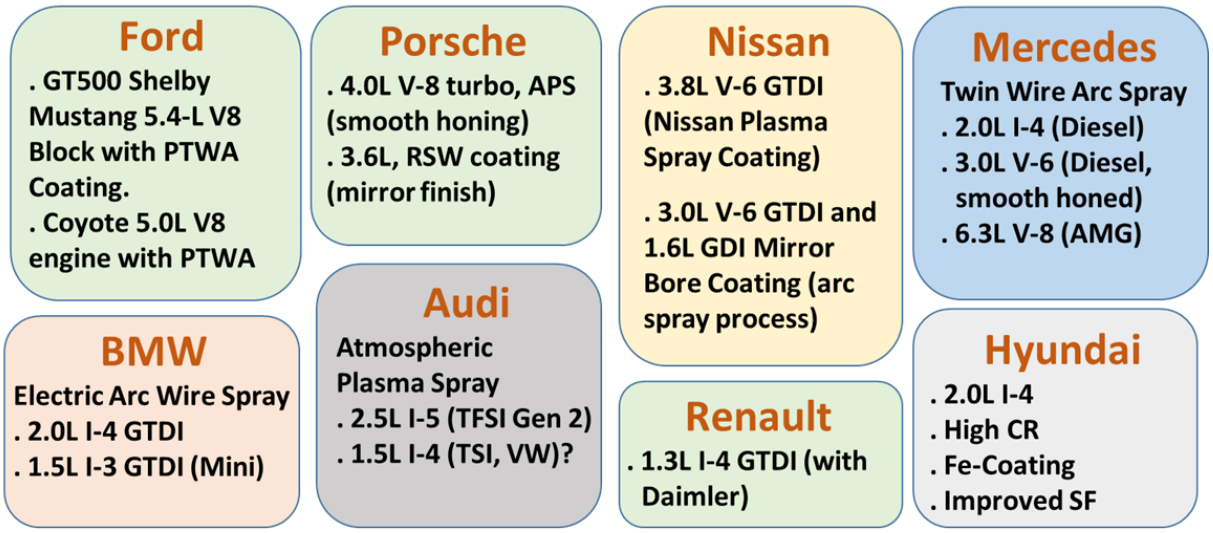

Figure 3. Industry landscape of thermal spray coating on automotive engines.

Bore Finish – Along with the high porosity PTWA coating, additional friction reduction benefit can be gained by improving the surface finish. Our recent investigations in a single cylinder motored engine test showed encouraging friction reduction opportunity with improved bore finish. Typical finish on cast iron liner in an engine is about 0.3-0.4 μm Ra. We target surface roughness down to below 0.2 μm Ra.

We estimate high porosity PTWA coating with improved bore finish will provide about 1.5% fuel economy benefit. The general concept of friction reduction is described schematically in Figure 4. Generally, as surface finish improves, coefficient of friction decreases. But there comes a point, where further decrease in surface roughness increases the coefficient of friction due to lack of oil availability on the surface as depicted by the red dotted line. However, if the surface contains pores serving as oil reservoirs, then the surface continues to be lubricated by the oil in the pores and the coefficient of friction can continue to go down.

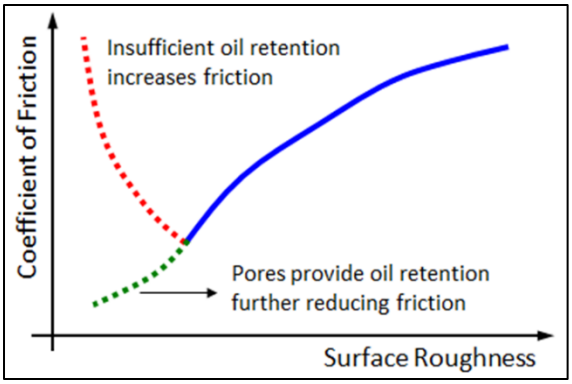

Figure 4. A schematic of friction reduction concept with surface porosity.

Piston Ring Coatings – In any tribological system, best friction and wear performances can be realized when both surfaces are optimized. In addition to improved finish with high porosity PTWA coating on cylinder surface, further friction reduction benefits can be obtained by using low friction coatings on piston rings. Presently Mo-NiCr filled top ring, nitrided second ring and cast iron oil control rings are used. Mo-NiCr coating is used primarily for improved scuffing performance, not necessarily for friction reduction. We investigated following coatings;

- PVD chromium nitride (CrN) - CrN is being used in some engines with cast iron liners for friction benefit but there could be synergistic effect with high porosity PTWA coating providing additional benefit. This coating is deposited by physical vapor deposition.

- Diamond-like carbon (DLC) - DLC coatings are known to offer low friction but the process for depositing DLC coating on piston rings is relatively new and is now available from several automotive component suppliers.
- Nitrided piston rings – Reducing the ring face contact area offers another way to reduce friction. This is also referred to as bullet nose design. The nitrided oil control rings with this design was included in this investigation.
- Nanocomposite coatings – Argonne National Laboratory developed VN-Cu and VN-Ni nanocomposite coatings were evaluated.

Piston Skirt – The original proposal included laser surface textures for friction reduction. However, discussions with piston suppliers, we learnt that minimal or no benefit was observed in their investigations. At present piston skirt has a solid lubricant coating and during laser texturing the coating is removed. The removal of solid lubricant coating risk piston scuffing (durability concern) and associated friction increase. Therefore, this technology was not pursued any further.

Bearings – In many engines today main and connecting rods use bored aluminum bearings. Also, polymer coated aluminum bearings are used on highly loaded engines. The original proposal included laying textures (laser dimples and laser lines) on main and connecting rod bearings for friction reduction. Again, following discussions with bearing suppliers it turned out that laser dimples or lines on polymer coated bearing is not feasible because of removal of polymer layer. Creation of dimples by mechanical means was not also considered feasible for the required size of these features for both coated and uncoated bearing within the current manufacturing process. Therefore, this application was not pursued any further.

Crankshaft – Main and connecting rod bearing friction can be reduced by micro-polishing (from current state of Ra – 0.10 μm to 0.04 μm) crankshaft journals with a consequent estimated fuel economy improvement of 0.25%.

Lubricants – During the proposal submission time, engine oils meeting minimum requirements of GF-5 specification was included. We developed novel polyalkylene glycol (PAG) based engine oil formulations, which showed significant friction reduction in motored valvetrain, engine, and chassis roll fuel economy tests under DOE award number DE-EE0005388 (8). We included this technology which is expected to provide an additional 1% fuel economy improvement.

Experience over thirty years suggests that the proposed target of 4% fuel economy improvement probably cannot be achieved by utilizing a single technology. A technology bundle as proposed above where each technology contributing a small portion has the highest potential to meet the stated target collectively.

2.0 SCOPE

The project scope was originally proposed to cover 3 years and included subcontract with Argonne National Laboratory (ANL). However, delays due to technical and COVID-19 related issues required periodic extensions to March 2021.

The objective of the proposed research is to develop and demonstrate friction reduction technologies for light, and medium, vehicles that improve fuel efficiency of future vehicles by at least 4% over currently (2015) used technologies based on comparative results from chassis dynamometer testing without adverse impacts on vehicle performance or durability. The objective will be achieved using new materials and low friction coatings, improved finish, design, and novel engine oil formulation.

Specifically, this project included:

- Development of low friction high porosity PTWA technology with mirror finished cylinder bore surface
- Low friction piston ring face coatings
- Polished crankshaft journals
- Low friction polyalkylene glycol (PAG) lubricant (a carry-over technology developed from a previous DOE project (DE-EE0005388))

The project is divided into three budget periods

Budget Period I: Deposition, characterization, and friction evaluation of high porosity cylinder coating and nanocomposite coatings for piston rings and piston skirt

In this first budget period, work initiated with exploring test conditions that will deposit high porosity PTWA coating with 1010 and 1080 wire feed materials at three porosity levels; <2%, 3-5%, and 6-8% with excellent control on process parameters and assessing initial friction characteristics. Also, nanocomposite coating development and deposition were initiated. Also, complete evaluation of friction and load carrying capability of textured connecting rod bearings was planned (but later discontinued as explained above).

Budget Period II: Friction and wear evaluation of PTWA coatings, piston skirts, and low friction ring coatings

In this budget period more detailed friction and wear characterization of PTWA and nanocomposite coatings were planned starting from laboratory bench tests to motored component level evaluations. This was initially expected with current production ring pack and then extended to other low friction ring coatings, piston skirts, and main and connecting rod bearings. Initiation of friction assessment in a fired single cylinder engine was planned.

Budget Period III. Multi-cylinder engine friction evaluation

This period was expected to focus on building engines with technologies showing the most promising friction and wear performances followed by friction evaluations on a motored engine and on a vehicle using the chassis roll dynamometer with GF-5 and PAG oils.

3.0 ACCOMPLISHMENTS

Accomplishments are described under each of the key tasks outlined in the project summary above. Although project management efforts were present throughout, this report will focus on technical achievements. The technical areas include high porosity PTWA coating development, and friction and wear evaluations on this coating and in conjunction with various ring coatings, and micro-polished cranks shafts using various test rigs.

3.1 PROJECT MANAGEMENT

Project management activities were completed in accordance with the Federal Reporting Checklist as well as special requests such as Annual Merit Review and on-site meetings.

3.2 TECHNICAL

3.2.1 EXPERIMENTAL DETAILS

3.2.1.1 High Porosity PTWA Coating Development

The coating development consisted of two parts, deposition and honing. A thermal spray process was used for coating deposition. The deposition was done using a spray torch, a schematic of which is shown in Figure 5. A plasma is struck between the cathode (torch) and the anode (wire feed stock) using a plasma gas consisting of a mixture of hydrogen and argon. The high heat generated at the plasma tip, melts the wire metal and the molten metal droplets are atomized and carried by the atomizing gasses toward the substrate where the material is deposited in layers. The plasma torch is rotated inside the cylinder bore and also traverses axially to deposit coating on the entire bore surface. Two types of wire materials are used in this investigation, 1010 wire which is a low carbon steel material, and 1080 wire which is a medium carbon steel material. The honing was done on free-standing aluminum and cast iron liners and cylinder bores using honing machine that are currently used in volume manufacturing.

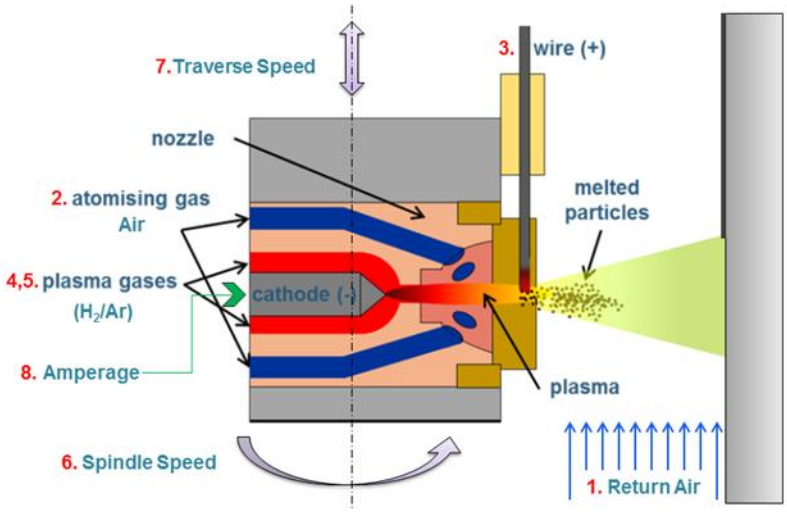

Figure 5. A schematic of thermal spray plasma torch used for high porosity PTWA coating deposition.

3.2.1.2 Coating Characterization

Hardness – Hardness was measured in Vickers scale using 500g load on the coating cross section with five indentations, spaced 20-25 μm apart.

Surface roughness – Surface roughness of coated bores was characterized by different methods; 2D stylus profilometry, 3D optical methods using NPFlex and NanoFocus machines.

Coating porosity – In the absence of any accepted standard, methods were developed using optical microscopy using Keyance microscope, and ImagePro software tool associated with an optical microscope. Also, software tools associated with NPFlex and NanoFocus were used. The results obtained

by these methods varied a lot depending on selection of different parameters and their levels. Correlation factors were established between different methods. The porosity values reported here are based on one particular measurement method and its equivalent using correlation factors developed for other methods. The porosity content on coupons and liners (following taking sections from it) were determined by directly putting them under the equipment mentioned above. However, for engine blocks, replicas of the bore surface were obtained for porosity analysis. High-resolution (resolution of 0.1 micron) fast curing two-part silicon rubber material (RepliSet-F5) from Struers was used.

Coating oxide content – Coating oxide content was determined (by area percent) using an optical microscope with ImagePro software tool, where the oxide phases on a polished sample was identified by its characteristic gray color.

Coating thermal conductivity – Thermal conductivity was measured using Flash Diffusivity Method using a coated disk of 10 mm diameter and 2 mm thickness. The measurements were done from room temperature to 400^{o}C. Once temperature inside the furnace is stabilized, a Xenon flash lamp is fired several times over a span of a few minutes on one side of the disk and the rise in temperature on the other side of the disk is measured (see Figure 6). The thermal conductivity is calculated using a standard equation.

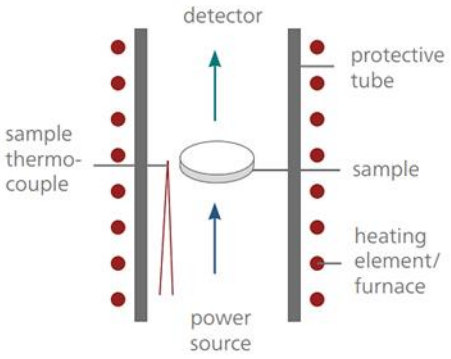

Figure 6. A simple schematic of principle of flash diffusivity method.

3.2.1.3 Friction Measurements – Friction measurements were conducted by following methods.

Laboratory bench tests: Reciprocating ring-on-liner – Plint TE-77 machine was used for boundary and mixed lubrication friction measurements where a ring section reciprocated against a fixed liner section using GF-5 SAE 5W-20 oil under following conditions enabling generation of Stribeck response

- Temp.: 30, 50, 80, 120°C
- Load: 50, 100, 150N
- Frequency: 2, 5, 10, 20, 30Hz

This procedure was developed to assess friction reduction potential of PTWA coatings and several ring face coatings i.e., production ring face coating (Mo-NiCr), physical vapor deposited chromium nitride coating (PVD CrN), and diamond-like carbon (DLC) coating.

A similar reciprocating machine developed by Argonne National Laboratory was used for measuring friction on nano-composite coatings against cast iron and PTWA coatings using the same test conditions. The nano-composite coatings were deposited on the top compression ring.

Laboratory bench tests: Reciprocating cylinder-on-flat – Friction measurements under boundary lubrication regime were conducted using a cylinder-on-flat contact geometry where both the cylinder and flat materials were made out of AISI 52100 steel. The flat reciprocated at 5hz with 6 mm stroke against a stationary cylinder held at 80N load (initial contact pressure 0.4 GPa) on its long axis at 100^{o}C oil temperature. This test configuration was used to evaluate the effectiveness of friction reduction of nano-composite coatings (VN-Cu and VN-Ni) developed by Argonne National Laboratory. The cylinder was coated.

Engine block preparation – Several liner-less aluminum engine blocks were produced by sand casting method for high porosity PTWA coating deposition and honing followed by friction and wear evaluations using cranktrain only and friction evaluations using full engine. The liner-less blocks were produced based on an existing high volume production inline four cylinder block architecture.

Motored single cylinder friction measurements – The single cylinder motored friction rig uses a floating liner technique. The architecture is based on one of high volume current production V-6 engines having a bore of 92.5mm, and stroke of 86.7mm. An image of the rig is shown in Figure 7. Production piston and connecting rod are used. The custom crank shaft has identical stroke and finish as the production engine. The aluminum liners press fitted on a cast iron sleeve had very low bore distortion, and are designed to 'float' as an assembly on an oil film allowing free vertical motion, which is extremely small. Forces are measured by three matched load cells. The entire engine and sealed carrier assembly has temperature controlled from 40^{o}C to over 100^{o}C to within roughly 1^{o}C by external oil heating and cooling systems. The engine is not pressurized. Data is reliable up to about 1750 rpm. For PTWA coating evaluation, individual aluminum liners were thermally press fit into carriers, spray coated and honed, and characterized for diameter and roughness. They were put into the rig and broken in, which involved operating the rig until the friction force data was stable. The rig captures friction of piston skirt and piston rings in contact with the liner. In this test while evaluating the effect of ring coatings the top compression and oil control rings had the same coating with a production second ring.

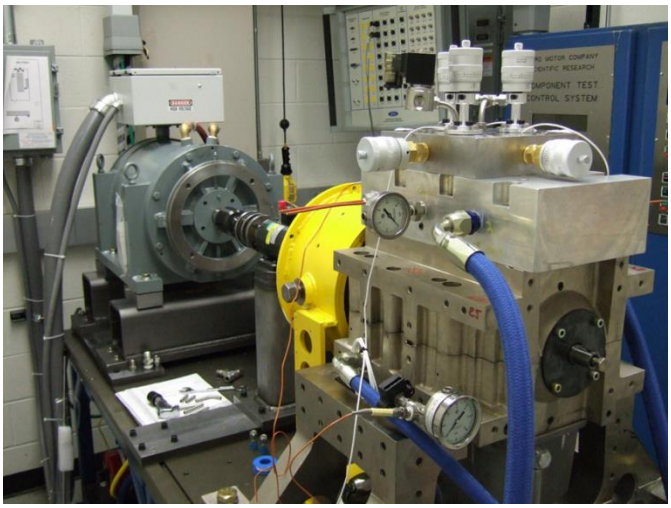

Figure 7. Motored single cylinder friction measurement assembly.

Motored cranktrain friction measurements – High porosity PTWA coated blocks are used for this investigation and the test rig is shown in Figure 8. The cranktrain assembly was carefully prepared ensuring a fixed piston-bore clearance of 32μm (diametrical) and nominal production bearing clearance. The engine is motored by a DC motor with an in-line torque transducer on the driveshaft. The temperature of the lubricant at the main oil gallery is controlled via a temperature controller for the closed lubrication circuit, which can be adjusted through a heater in an oil reservoir. Using fluid bypass valves, the interaction between frictional dissipation and local thermal conditions is controlled for low temperature tests. This minimized the influence of the rapid change in thermal conditions at the rubbing surfaces on bulk oil temperature. A water-glycol mixture was also circulated through the original channels in the block for faster temperature equilibrium.

Figure 8. Motorized cranktrain assembly.

Friction contributions at interfaces between piston skirt/liner, piston ring/liner and bearings (main and con rod) are captured in this test. In this test while evaluating the effect of ring coatings the top compression and oil control rings had the same coating with a production second ring.

The moving surfaces in the block were broken-in by running the rig 600 RPM-4000 RPM for various length of time until friction readings are stabilized. This procedure can take 175 to 300 hours. The friction performance was evaluated between 600 and 4000 r/min at oil temperatures of 40^{o}C, 60^{o}C, 100^{o}C and 120^{o}C. Before each test, the engine is motored at 1000 r/min and electrical heaters are used to provide an additional heat input for the target temperatures above 40^{o}C. For tests at 40^{o}C, friction heating alone is sufficient to achieve the temperature target and fluid bypass valves are operated to ensure temperature stability during testing at high engine speeds. The friction test is repeated for two or more times at each target temperature for statistical purposes and data validation. The average of such measurements are reported. When changing to new oil, a lubricant flushing process is carried out, where the engine is (a) filled with the oil to be tested, (b) run engine 600 to 1500 r/min for sixty minutes, (c) drained, and (d) refilled with a new batch of the oil to be tested. A new oil filter is also installed after oil drain. Motoring torque, engine speed, oil pressures, oil and coolant temperatures at different locations are recorded by a data acquisition system (National Instruments LabView) with a sampling rate of 6 Hz.

Micro-polishing of crankshaft – Main and connecting rod journals of an in-line four cylinder production engine (the same engine used for other friction and wear tests) were micro-polished with finer grits. Detailed surface finish inspection was conducted following micro-polishing. The micro-polished crankshaft was assembled on the engine block for friction assessment using the motored cranktrain friction rig without the pistons and connecting rod. Therefore, only main bearing friction was recorded.

Motored engine friction measurements – Several engines were built was high porosity PTWA coated blocks maintaining 45μm (diametrical) piston-bore clearance and nominal production bearing clearance. The engines were first broken in at peak torque at 2000 rpm for 100 hours followed by about 150 hours of motoring to ensure a stable friction response at each of the engine speed investigated. Friction measurements under each condition is repeated five times and the average of such measurements are reported. SAE 5W-20 GF-5 engine oil was used and supplied from an external sump maintained at 35^{o}C, 60^{o}C, 90^{o}C, and 120^{o}C. The coolant was maintained through the block and its temperature was also controlled at appropriate level.

Fired single cylinder friction evaluation – Ricardo Hydra single cylinder naturally aspirated indirect injection research engine with 86 mm bore was used. The engine is modular in nature and a removable cast iron sleeve is inserted into the block. External sumps and pumps allow tight control of delivery pressure and temperature of the test lubricant essential to ensure measurements are taken at the same lubricant viscosity. Fuel pressure is also controlled to ensure consistent fuel delivery to the engine. Inlet air is also temperature and humidity controlled to ensure consistent combustion. Piston assembly (piston and rings) friction is measured using strain gauges attached to the side of the connecting rod. These are set up as a Wheatstone bridge that cancels out any bending of the rod and amplifies the compression and tension the rod experiences during operation. This in itself is not sufficient to obtain the true frictional data as the forces on the piston assembly need to be accounted for, these primarily being combustion pressure and inertia. These forces are resolved per half crank angle as the connecting rod changes angle with the piston position. A pegging transducer is located on the side of the engine liner and this is exposed to the combustion chamber as the piston reaches 110 degrees after top dead center. This pegging transducer is used to recalibrate the combustion pressure transducer each engine cycle. 33 consecutive engine cycles are recorded at 250 kHz for each friction measurement. These 33 measurements are aligned by the software at TDC pulse and the correct number of measurements checked for. The Coefficient of Variance of the engine power across the 33 cycles is then calculated and only those below 5% are accepted. Multiple measurements at each engine speed and load condition are taken during testing to maximize the chance of an acceptable measurement being recorded. The wires containing the signals from the strain gauges are routed out of the engine using a grasshopper linkage, as shown in Figure 9. Extreme care was exercised during engine assembly to minimize friction torque variation and this includes head bolt torque, rod bearing cap torque, timing belt torque, and precise location of pressure transducer. The lubricant used was GF-5 SAE 5W-20 oil.

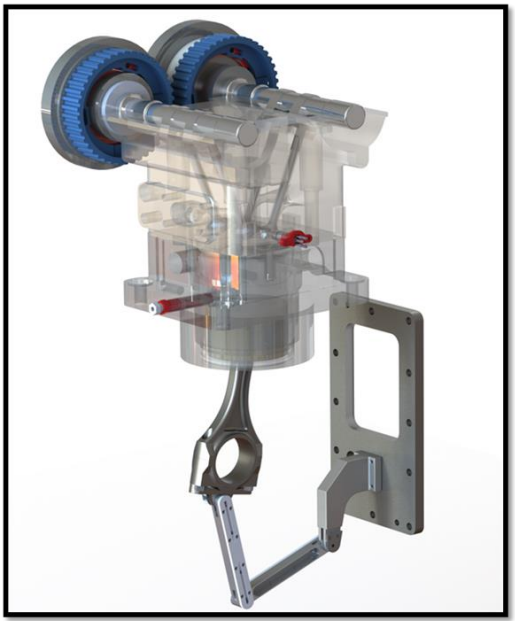

Figure 9. Grasshoper linkage for measuring friction force.

The friction force was measured at load-speed points shown in Table 1. Prior to friction testing, all the piston/ring/liner sets were assembled in the engine and operated for 60 hours at medium speed and load to run-in liner and ring surfaces.

Table 1. Engine speed and load points used for friction measurements.

Test point	Speed (rpm)	Target Load (Hp)
1	1500	1.5 (Low)
2	1500	2.1 (Medium)
3	1500	5.8 (High)
4	2000	2.7 (Low)
5	2000	5.0 (Medium)
6	2000	8.0 (High)
7	3500	4.0 (Low)
8	3500	7.4 (Medium)
9	3500	15.5 (High)
10	5000	4.2 (Low)
11	5000	15.5 (Medium)
12	5000	19.8 (High)

3.2.1.4 Cylinder Bore and Piston Ring Wear Measurements - The wear behavior of cylinder bore and piston ring materials was assessed with the use of a motored cranktrain rig coupled with radionuclide technique. The rig used an inline four cylinder engine short block. The cylinders were open to the atmosphere. The crankshaft was driven by a 15 hp motor. Heat was provided externally, with the use of a heating tank for the coolant, and an inline heater for the engine oil. With the radionuclide technique, the wear measurement was conducted on one activated component at a time. Fundamentally, as the piston rings slide against the cylinder bores, radioactive wear debris is generated from the activated component, which gets mixed in the oil. The wear measurement system uses an external pump to circulate engine oil from the engine sump, through two radiation detectors and the inline oil heater, and then back to the sump. The first radiation detector measures the radioactivity in the oil, and the second radiation detector measures the radioactivity in the oil filter. The software converts radioactivity to mass loss in real time. An image of the rig set up is shown in Figure 10.

Cylinder bore wear behavior was compared for a current production engine block with cast iron liners and a high porosity PTWA-coated engine block. The high porosity PTWA-coated block was produced from an AISI 1080 steel wire. The surface of cylinder 3 was activated with Co^{56}. The activated area was a 360 degree band of 12 mm width near top dead center. The depth of the activated surface was about 20 μm, which was greater than the expected wear depth. The wear resistance of cylinder bores was evaluated against current production, CrN PVD, and DLC-coated ring packs, as shown in Table 2. The candidate ring coatings were only installed in the activated cylinder. The candidate coatings were applied to the upper compression ring and the oil control ring, but not to the lower compression ring. The coated ring packs were run first in the cast iron block, and then re-used in the PTWA-coated block. The same set of current production rings were used in all non-activated cylinders for all bore wear assessments.

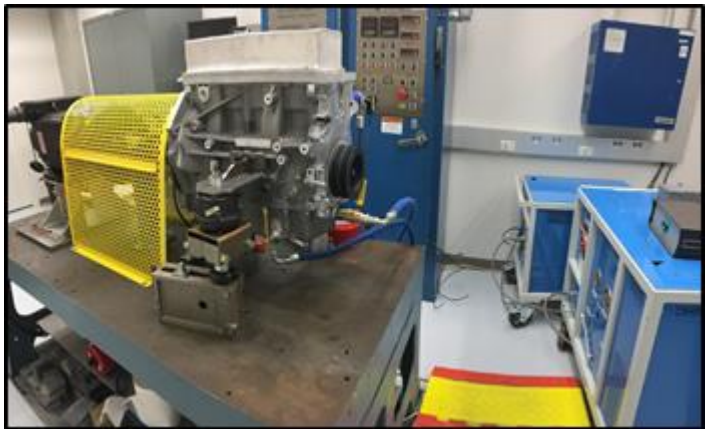

Figure 10. The set up for motored cranktrain wear rig.

Table 2. Bore wear test matrix

Test #	Cylinder bore material	Isotope of bore	Ring pack coating
1	Cast Iron	Co56	Current production
2			PVD CrN
3			DLC
4			Current production
5	PTWA	Co56	PVD CrN
6			DLC
7			Current production

Piston ring wear was compared for current production rings (nitrided steel), CrN PVD rings, and DLC-coated rings. The surface of the oil control ring face was activated along the full axial width of both rails. The isotope depended on the chemical composition of the coating, as shown in Table 3. The depth of the activated surface was about 20 μm for nitrided steel and CrN PVD rings, and 1 μm for DLC-coated rings due to its thin coating. The wear behavior of piston rings was evaluated against cast iron and high porosity PTWA-coated cylinder blocks.

Table 3. Piston ring wear test matrix

Test #	Cylinder bore material	Isotope of bore	Oil control ring coating
9	PTWA	Be-7	DLC
10		Co-56	Nitride steel
11		Cr-51	PVD CrN
12	Cast Iron	Be-7	DLC
13		Cr-51	PVD CrN
14		Co-56	Nitride steel

Each engine short block was built with select fit pistons to maintain a 32 μm piston-to-bore clearance. Fresh SAE 5W-20, GF-5 quality oil was used in all wear assessments. The engine oil and coolant temperature were maintained at 100°C. The wear test cycle is shown in Figure 11, in which engine speed was quickly cycled between 750, 2000, 2500, and 3500 rpm to promote wear. Prior to wear measurements, each new engine block was broken-in by repeating the test cycle for about 150 hours. For wear evaluations, the test cycle was repeated for at least 75 hours, in which the first 20 hours were considered an additional break-in period for piston rings, and steady state wear rate was determined from the final 55+ hours.

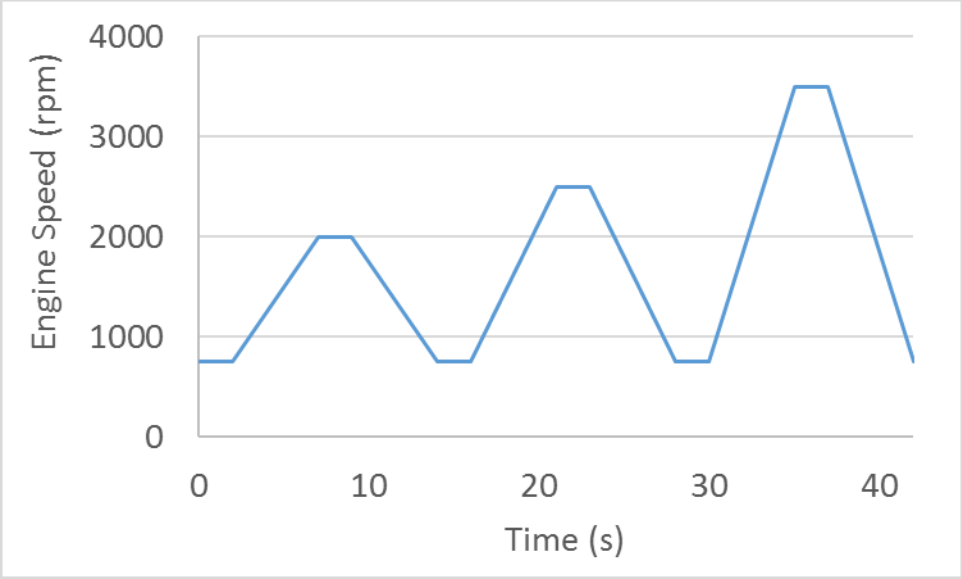

Figure 11. Test cycle used for wear evaluations.

In addition to wear, cranktrain friction torque was measured by an in-line torque meter. The main sources of friction were from the power cylinder components and crankshaft. After completion of each wear evaluation, a speed sweep was run to assess friction torque. The speed sweep included engine speeds of 750, 1000, 1500, 2000, 2500, and 3500 rpm. The speed was held constant for 30 minutes at each speed step. The average friction torque at each speed was recorded.

3.2.1.5 Chassis Roll fuel Economy Tests – The chassis roll fuel economy was measured on a small sport utility vehicle with an inline four cylinder engine, the same engine used for motored engine friction evaluation. The engine was built with a technology bundle consisting of liner-less high porosity PTWA coating (PTWA3b), polished crank journals, and DLC-coated top and oil control rings. The engine was already broken in from previous friction tests. The engine oil used for this engine were SAE GF-5 5W-20 and polyalkylene glycol (PAG) oils. The PAG oil 15-1 was developed from a previous DOE funded project (8) and showed significant friction reduction benefit. The results from the coated blocks were compared against a same production engine with cast iron liners and production ring and crankshaft with factory fill GF-5 SAE 5W-20 oil. Eight to ten tests were conducted under each engine configuration. Before changing PAG oil, the SAE 5W-20 oil was drained from the engine and flushed twice with PAG oil.

3.2.1.6 Lubricants – Two lubricants were used in this investigation, GF-5 SAE 5W-20 oil and polyalkylene glycol designated as PAG 15-1. The polyalkylene glycol was used only in two sets of experiments; cranktrain friction with polished crank journals, and chassis roll fuel economy tests. The properties of the two fluids are shown in Table 4 below.

Table 4. Physical properties of lubricants

Properties	GF-5 SAE 5W-20	PAG 15-1
Viscosity at 40^{o}C (cSt)	48	20.3
Viscosity at 100^{o}C (cSt)	8.6	5.5
VI	164	232
High Temp high shear viscosity at 150C (cP)	2.6	2.7

In addition, two other engine oils were also used; Mobil 1 SAE 5W-20, which is a synthetic oil and an used oil (GF-5 SAE 5W-20). The used oil was collected from a Ford Management Lease vehicle with 10,000 miles on it. These two oils were used in laboratory bench tests at Argonne National Laboratory to get an initial assessment on the effects of oil formulation and aging on friction.

3.2.2 RESULTS and DISCUSSION

3.2.2.1 Nano-composite Coating

Figure 12 shows a comparison of coefficient of friction observed with VN-Ni nano-composite coating with Mobil 1 and GF-5 SAE 5W-20 oils. In the presence of GF-5 SAE 5W-20 oil, the coefficient of friction observed with VN-Ni coating was comparable to uncoated steel at the end of one hour test, while Mobil 1 showed about 25% reduction. Mobil 1 did not show any reduction in coefficient of friction with uncoated AISI 52100 steel suggesting possible synergistic effect between Mobil 1 lubricant and nano-composite coating.

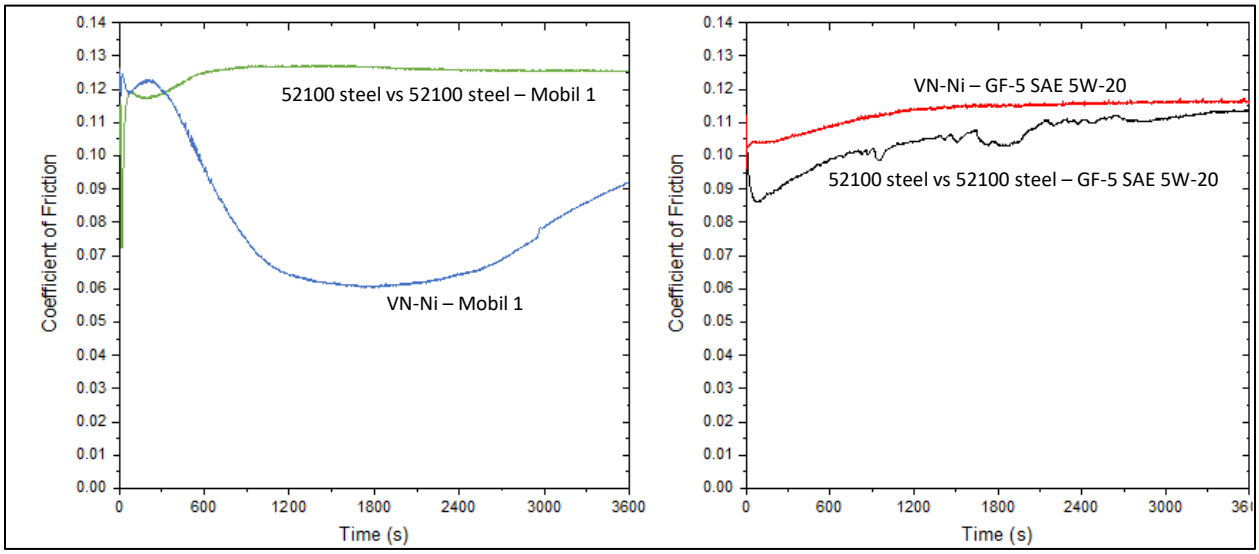

(a) (b)

Figure 12. A comparison of coefficient of friction between uncoated and nano-composite VN-Ni coating against GF-5 SAE 5W-20 and Mobil 1 oils.

Figure 13 shows optical microscope images of wear scar on cylinders with and without coating with both oils. A distinct wear scar could be observed on uncoated AISI 52100 steel cylinders with both oils while

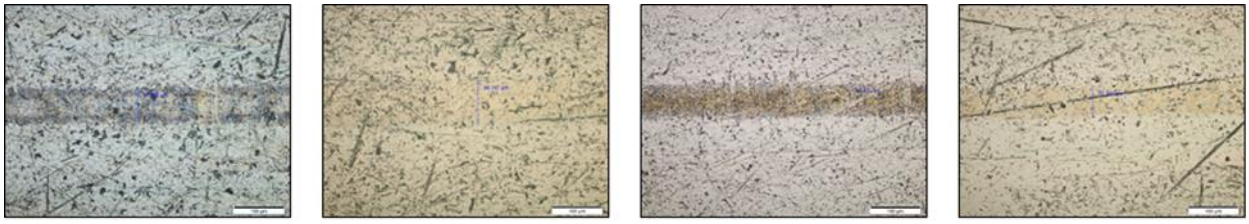

(a) (b) (c) (d)

Figure 13. Optical microscope images of wear scar on AISI 52100 steel cylinders. (a) uncoated with Mobil 1, (b) VN-Ni coated with Mobil 1, (c) Uncoated with GF-5 SAE 5W-20, and (d) VN-NI coated with GF-5 SAE 5W-20.

the wear scars on VN-Ni coated cylinders are relatively faint indicating a comparatively less wear demonstrating improved wear resistance.

Stribeck-like curves were generated by collecting friction data during one minute at different reciprocating frequencies (ranging from 24Hz to 0.1 Hz) to evaluate the performance of the VN-Ni coating under different sliding regimes. The results in the graph below show that, the VN-Ni coating provided lower coefficient of friction (COF) across all speed ranges when tested in Mobil1 oil compared to GF-5 SAE 5W-20 oil. The COF under lower speeds (under boundary lubrication regime) shows the higher benefit of the coatings in the presence of Mobil1 oil. (Figure 14).

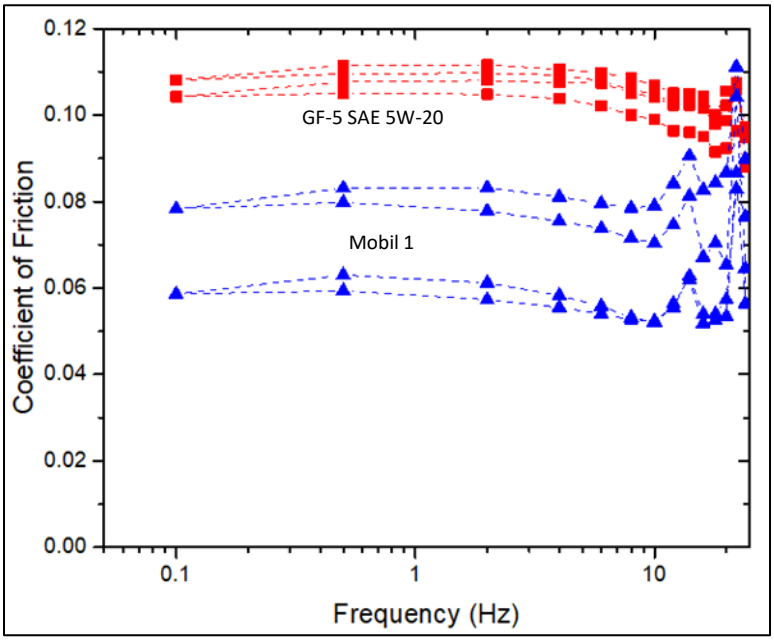

Figure 14. Coefficient of friction of VN-Ni coated surface on different reciprocating frequencies (speeds).

The effect of vehicle aged oil on coefficient of friction of VN-Ni and VN-Cu nano-composite coatings was evaluated and the results are shown in Figure 15. The test conditions were slightly different to make it more severe. The load and the test duration were increased to 350N (initial contact stress 1GPa) and six hours respectively. The VN-Ni and VN-Cu coatings show smaller wear scars and the coefficient of friction is reduced at least by 15% in the case of VN-Cu coating compared to uncoated steel.

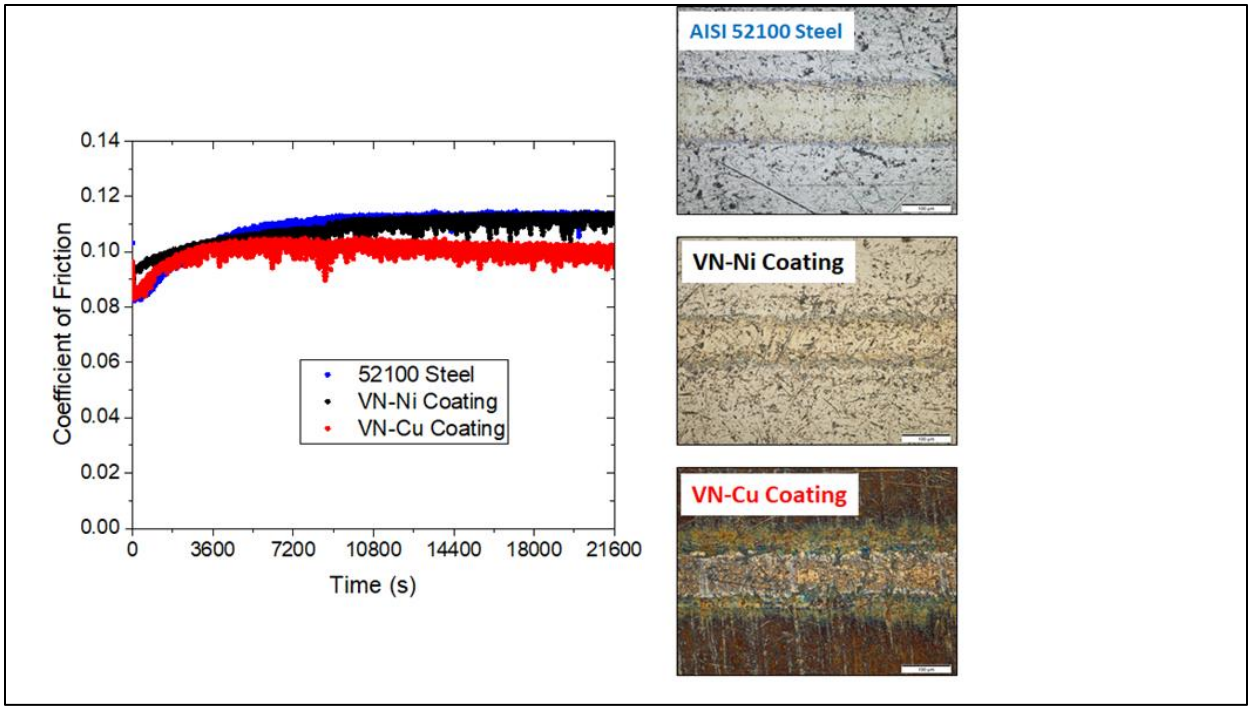

Figure 15. Coefficient of friction and optical images of VN-Ni, and VN-Cu coated and uncoated cylinders showing wear damage in sliding contact areas.

To better understand the VN-Cu coating performance as a function of sliding speed in the presence of new and vehicle aged oils, a ball-on-disc contact geometry was used where a 9.5 mm diameter ball made of AISI 52100 steel was pressed against a rotating disk made of the same material under 10N load (initial contact stress 1 GPa) at 100^{o}C oil temperature. The results are shown in Figure 16 where VN-Cu coating shows lower coefficient of friction with vehicle aged oil than fresh oil while uncoated AISI 52100 steel showed similar coefficient of friction with both oils.

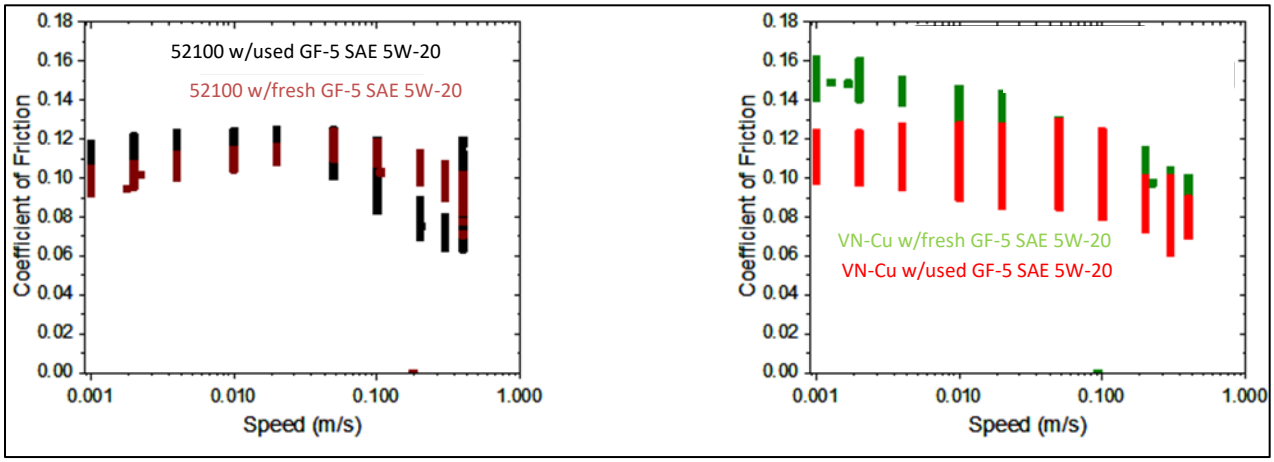

Figure 16. Coefficient of friction of uncoated and VN-Cu coated surfaces with fresh and used GF-5 SAE 5W20 oils as a function of speed.

3.2.2.2 High Porosity Coating Development – The high porosity coating development was initiated with Comau Inc because of their knowledge and deep understanding of the process and also being a supplier of PTWA coating applied on one of Ford's high volume engines. The objective was to create three levels of porosity (a) PTWA 1 (less than 2%), (b) PTWA 2 (3-4%), and (c) PTWA 3 (6-8%). The production coating

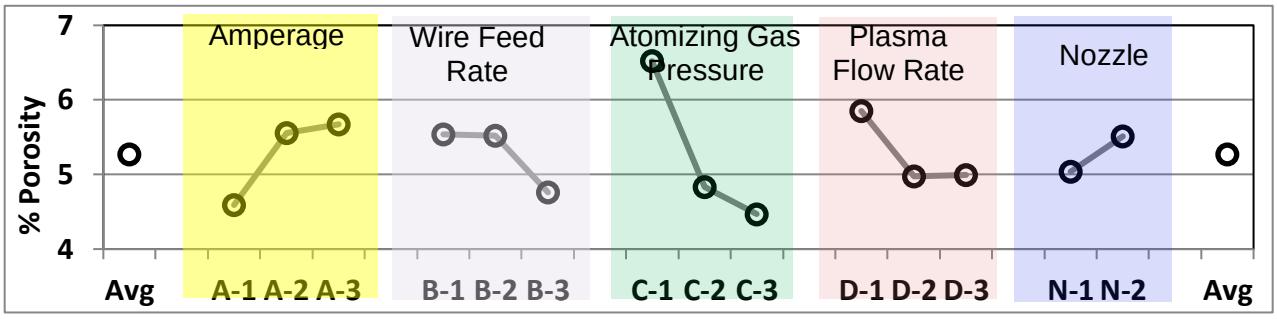

Figure 17. Key coating deposition parameters.

has low porosity and did not offer any friction advantage. The development of high porosity PTWA coating initiated with deposition on 25 mm square steel coupons and measuring porosity on the cross section of the coating following metallographic polishing. The objectives of this exercise were two folds; (a) get a better understanding and identification of key coating deposition parameters, and (b) develop a method for porosity measurements. There are several coating deposition parameters that are controlled and monitored such as (a) return air being on or off, (b) air pressure, (c) wire speed, (d) amount of hydrogen, (e) plasma gas flow rate, (f) spindle speed, (g) traverse speed, (g) amperage etc. Initial trials with three different nozzle designs did not produce significant increase in porosity levels. Porosity level for all three designs was ~1%, leading to further evaluations of torch parameters and nozzle modification. A factorial design of experiments (DOE) on coupons identified wire feed rate, spindle traverse speed and atomizing gas pressure play key roles in controlling porosity. Based on these encouraging results, the next step was to move forward with coating on 83 mm diameter aluminum liners. The coating deposition parameters needed revisiting as the substrate geometry changed from flat coupons to liners. Another fractional DOE was conducted to identify key parameters and their levels. Cross sectional porosity measurements on 83 mm liners helped identifying key coating deposition parameters. The results are shown in Figure 17 with porosity levels measured on the cross section of liners. Wire feed rate, amperage, atomizing gas pressure, and plasma gas flow rate are identified as key parameters with their respective levels resulted in coatings porosity levels ranging from 0.2 to 6.5%. Additionally, a new nozzle designed to reduce particle speed appeared to have a positive effect on porosity.

There were several steps involved in liner development and Figure 18 shows a schematic of work flow. The aluminum liners were mechanically roughened to aid in mechanically interlocking coating on the

surface. Cast iron liners were also coated for use in fired single cylinder rig, for which the surface preparation step involved depositing a bond coat first prior to depositing PTWA coating.

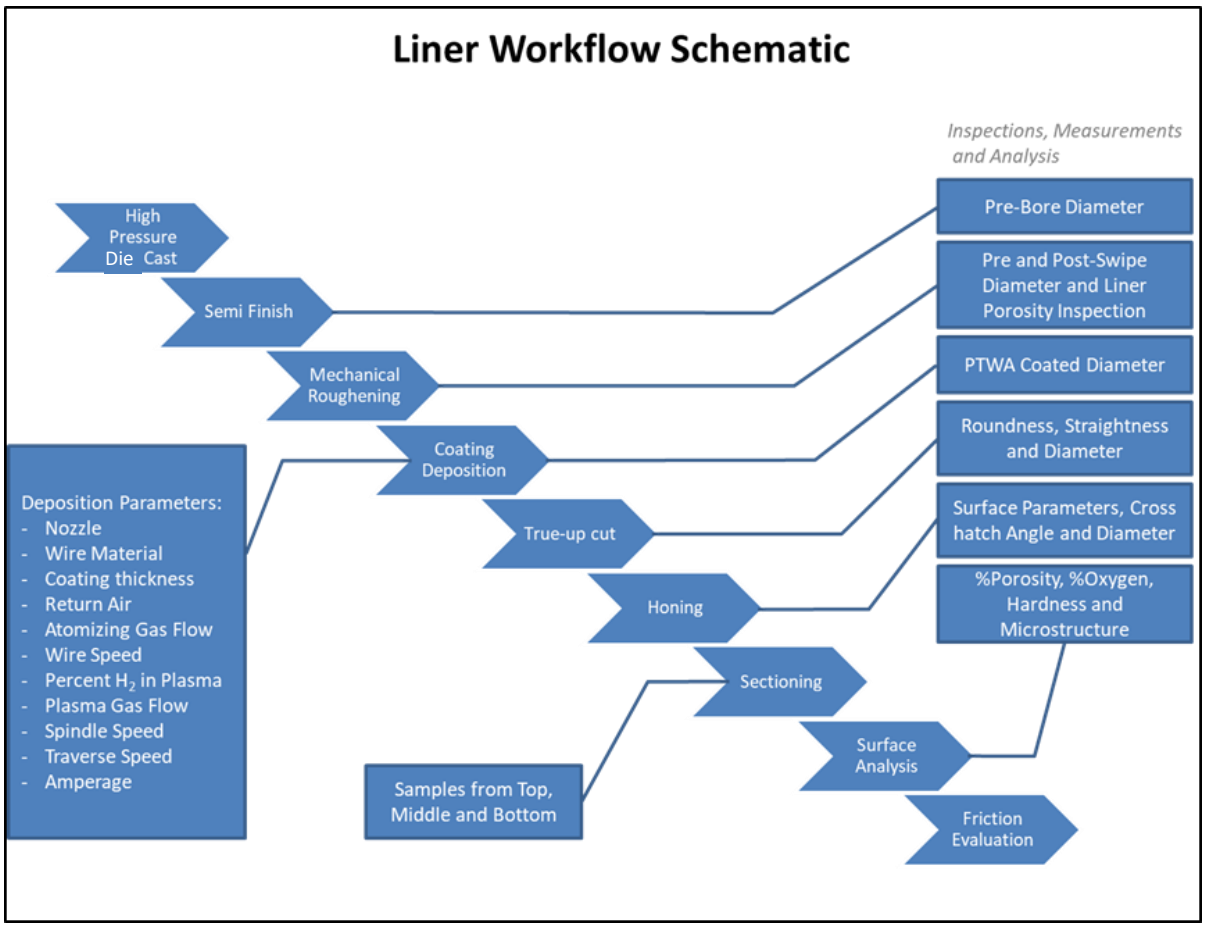

Figure 18. A schematic of work flow for PTWA-coated finished liner for friction evaluation.

Figure 19 shows porosity distribution on coating cross section. Also shown in the figure the mechanical surface roughening geometry (the wedge) to hold coating on the surface. The coating is generated in layers as shown by the curved interfaces. The coating also contained pores indicated by dark black regions, and oxide phases as shown by gray regions. However, porosity on the surface of the liner is considered more important for friction reduction than on the cross section. Measurement on the liner surface revealed much lower porosity level than on the cross section as shown in Figure 20. The porosity level was only 2.3% while cross section results showed 5.5%. Figure 21 shows a weak correlation between cross sectional porosity and liner surface porosity. Therefore, attention was focused on honing.

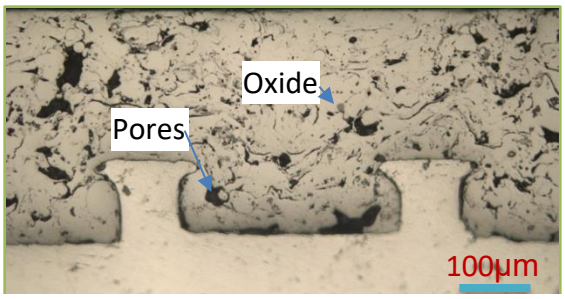

Figure 19. Porosity distribution on coating cross section.

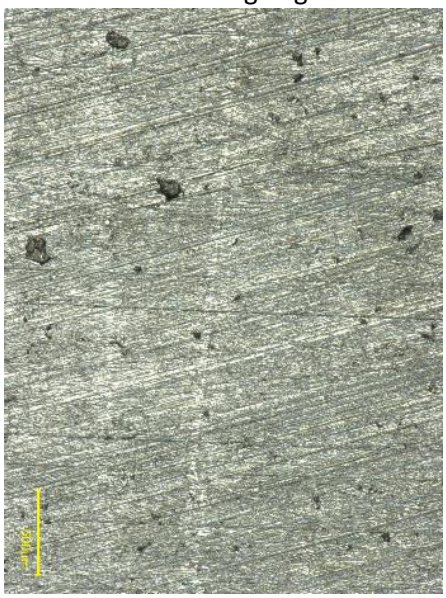

Figure 20. Liner surface porosity distribution and its level.

Honing played a critical role in increasing porosity level by exposing more pores on the coating surface. A detailed investigation was carried out by varying conditions at different honing steps. It turned out that there are three mechanisms of pore generation as shown in Figure 22. Naturally occurring pore generates during coating deposition due to air entrapment. Additionally, during honing, delamination of thin spat layers very near to the surface creates pore as shown in Figure 22(b). There are also partially molten particles not bonded strongly to the coating matrix are removed creating pores.

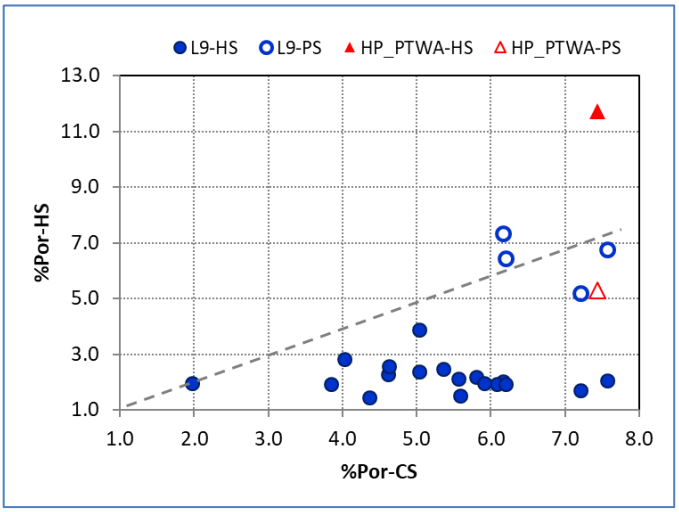

Figure 21. Lack of correlation between porosity measured on cross section (CS) and hones surface (HS) for high porosity (HS PTWA coatings. Data includes from L-9 factorial DOE.

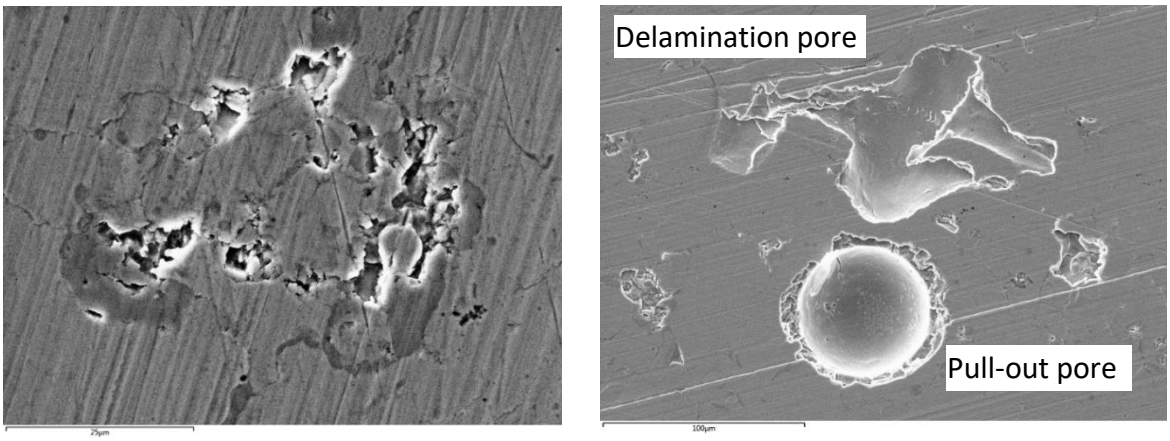

(a) (b)

Figure 22. Sources of pore generation during (a) coating deposition, (b) honing by delamination and pull out

A similar DOE was conducted for depositing coatings on 92.5 mm diameter liners to ensure the process is robust enough to apply on liners of different sizes and engine blocks. The key parameters and their effects on porosity level were similar to those found with DOE with 83 mm diameter liners. The DOE also included wire material composition as a variable to understand its effect on porosity generation. It was observed that 1080 material with nitrogen as atomizing gas resulted in higher porosity than 1010 wire material.

The honing process optimization created desired porosity levels and also produced a mirror finished surface. Figure 23 shows the range of porosities produced on the honed surface and the ability to tune in a desired level through the developed optimized coating and honing conditions. Figure 24 shows the distribution of pores on honed surface. Porosity levels were divided into various groups as follows

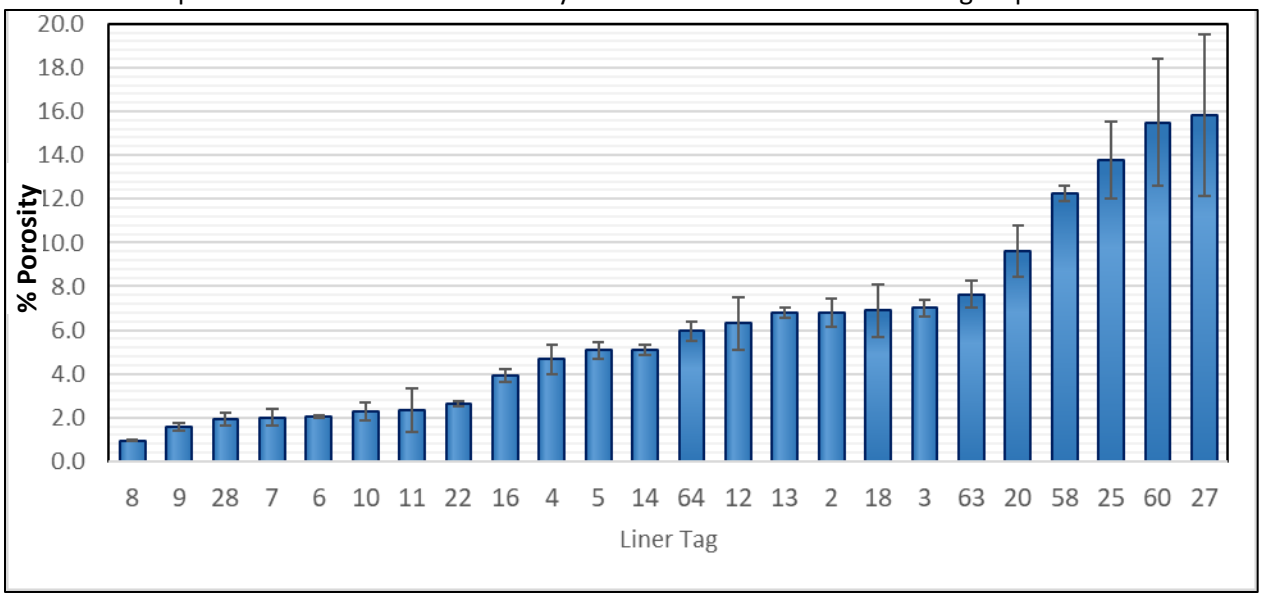

Figure 23. Process optimization helped in tuning in to a wide range of porosity levels.

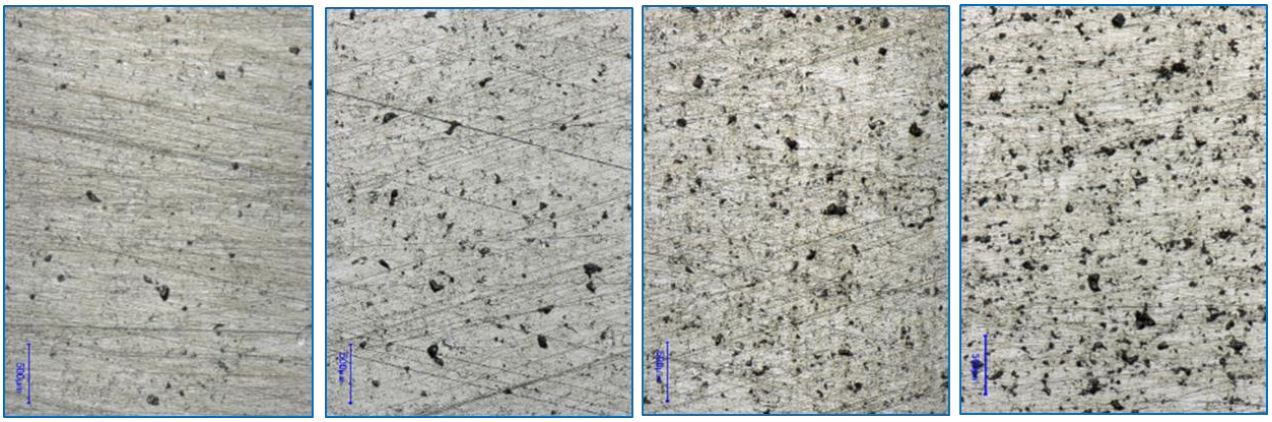

(a) (b) (c) (d)

Figure 24. Image of honed surface showing different levels of porosities (a) PTWA1 (less than 2%), (b) PTWA2 (3-5%), (c) PTWA3 (6-8%), (d) PTWA4 (>8%).

PTWA1 (less than 2%), PTWA2 (3-5%), PTWA3 (6-8%), and PTWA4 (>8%).

Several engine blocks were coated for friction evaluation using motored cranktrain and motored engine with the optimized coating and honing parameters with different porosity levels. However, porosity analysis on surface replica taken from bore surface showed lower than desired levels but fortunately meeting targeted values. This raised a big concern. Upon thorough investigation on coating deposition and honing parameters, it was identified that the torch used previously was not available and a different torch was used. As part of a root cause analysis all the torches at the supplier were analyzed and re-evaluated to establish part by part variation. The most promising torches were identified and used in an L9 DOE analysis on coupons to re-establish the parameters focusing on wire material 1080 and nitrogen atomizing gas. High porosity levels were achieved on polished coupon cross section but much less was observed when the same coating deposition parameters were used on honed surface of liners. This exercise clearly highlighted the importance of torch design for creating high porosity. Therefore, the focus was shifted on honing parameters. A detailed investigation was conducted again with various honing conditions and also extending honing steps. The team spent great efforts and finally succeeded in identifying a five-stage process revealing nearly 8% pores on honed surface. The new process was applied for coating cast iron liners for fired single cylinder friction evaluation.

3.2.2.3 Coating Characterization

Oxide content - The oxide content on the coating was quantified using the ImagePro software in an optical microscope and examining the coating cross section. The oxide content varied from 7.5% to 13.8% depending on coating deposition conditions.

Hardness - The coating hardness is measured on coating cross section and the results are shown in Figure 25. The hardness did not vary significantly with porosity level but wire material 1080 showed a little higher hardness than wire material 1010 and this is simply because of slightly higher carbon content on 1080 material. In comparison, the hardness of cast iron liner material is about 311Hv.

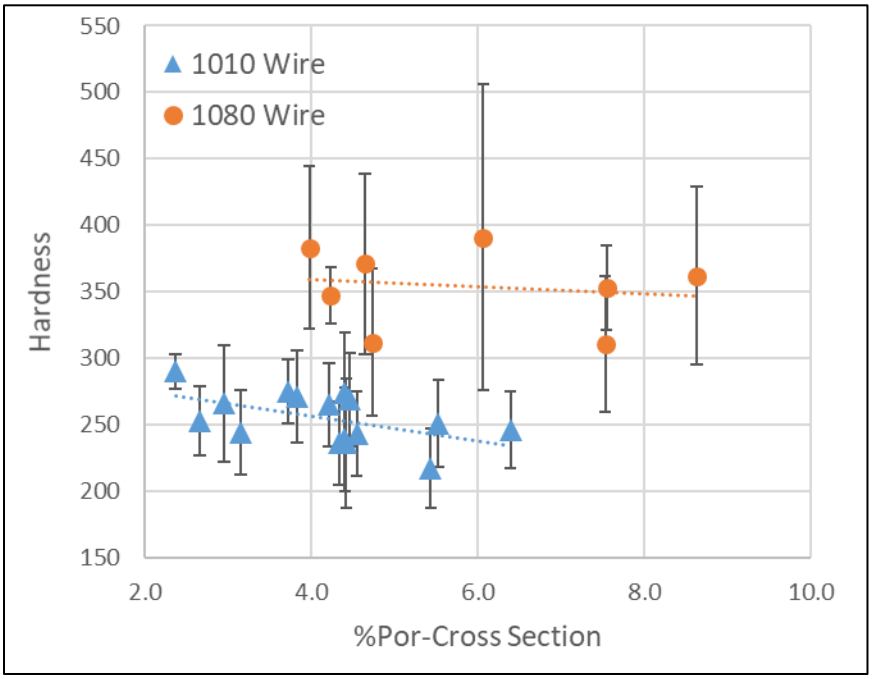

Figure 25. High porosity PTWA coating hardness is influenced by wire material composition.

Surface finish – The surface roughness of liners following coating deposition and honing was conducted using 3D optical (NanoFocus) technique. Figure 26 shows various surface roughness parameters of mirror-finished honed surface based on more than one hundred measurements on four porosity levels. PTWA3a and PTWA3b refers to two different PTWA coatings falling on the same group and the porosity level of PTWA3a is at the lower range of the group and PTWA3b is at the higher end of the group. The measurements include pores, therefore, higher the porosity level higher the values of roughness parameters. The surface roughness parameter Sa was calculated without considering pores for various porosity levels and compared with cast iron liner surface as shown in Figure 27.

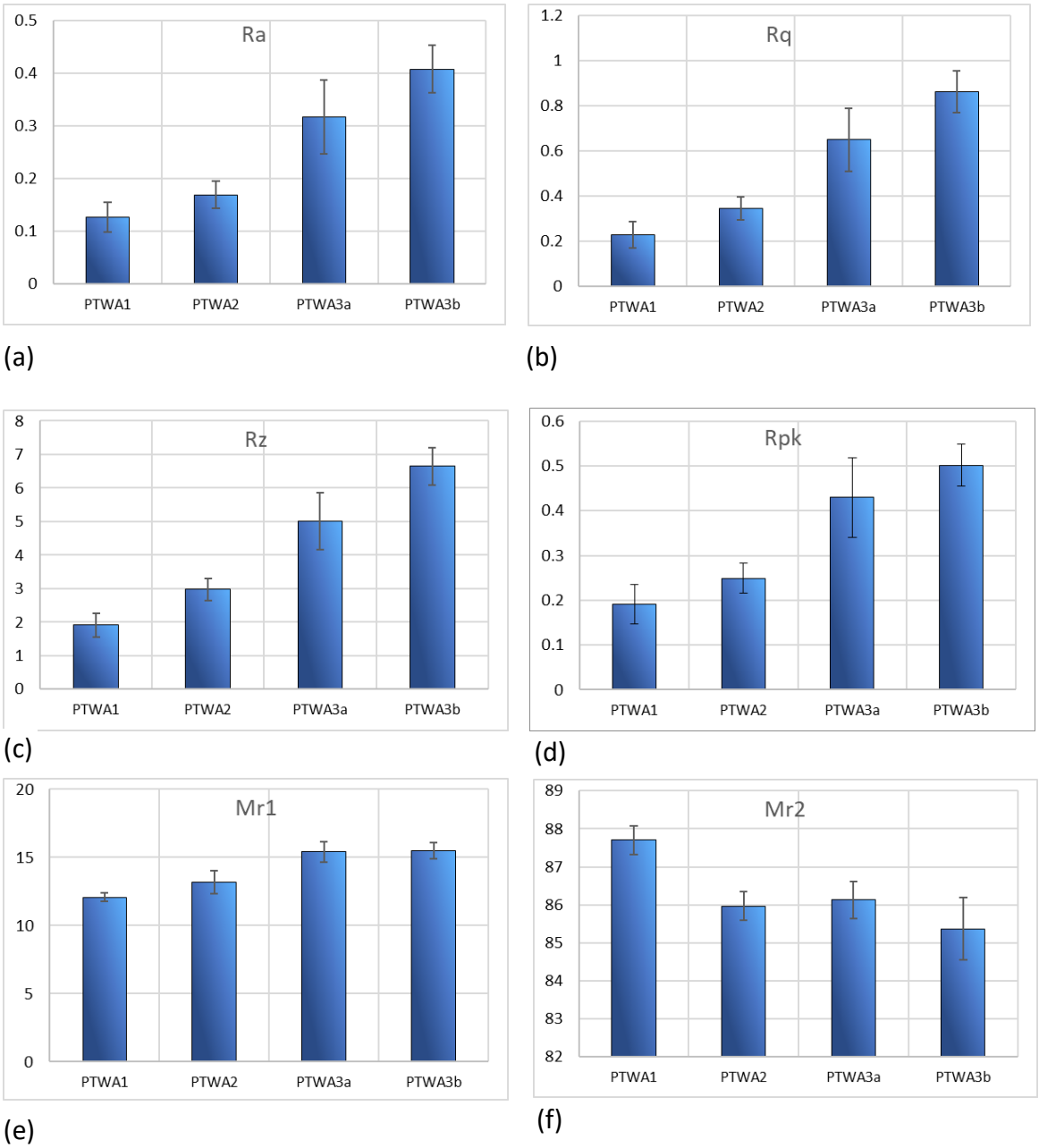

Figure 26. Surface roughness parameters of honed surfaces. (a) Ra, in μm, (b) Rq in μm, (c) Rz in μm, (d) Rpk in μm, (e) Mr1 I %, and (f) Mr2 in %. PTWA 3a and PTWA3b refer to two different porosity levels in the same group.

The NanoFocus machine also calculates the pore area and pore density by classifying pore into different sizes; Class1 (10-50 μm^2), Class2 (50-100 μm^2), Class3 (100-250 μm^2), Class4 (250-500 μm^2), Class5 (500-1000 μm^2) and Class6 (>1000 μm^2). Figure 28 shows pore size ranges and pore density for PTWA coatings at different porosity levels. Obviously, the larger pores contribute more to pore area as shown by the increasing slope from Class1 to Class6. Also, the curves mostly run parallel as porosity level increased

indicating no significant change in size distribution. However, pore density indicates there are more small pores than large pores on the surface.

Thermal conductivity – The thermal conductivity and specific heat of PTWA coatings with various porosity levels are shown in Figure 29 as a function of temperature. The thermal conductivity decreased slightly with temperature and did not change significantly with the porosity levels. In general, PTWA coatings showed lower thermal conductivity than cast iron. The specific heat of

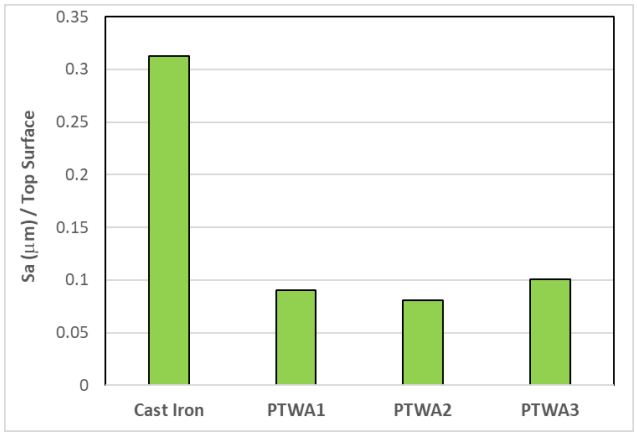

Figure 27. The surface finish of high porosity PTWA coatings excluding pores on the surface.

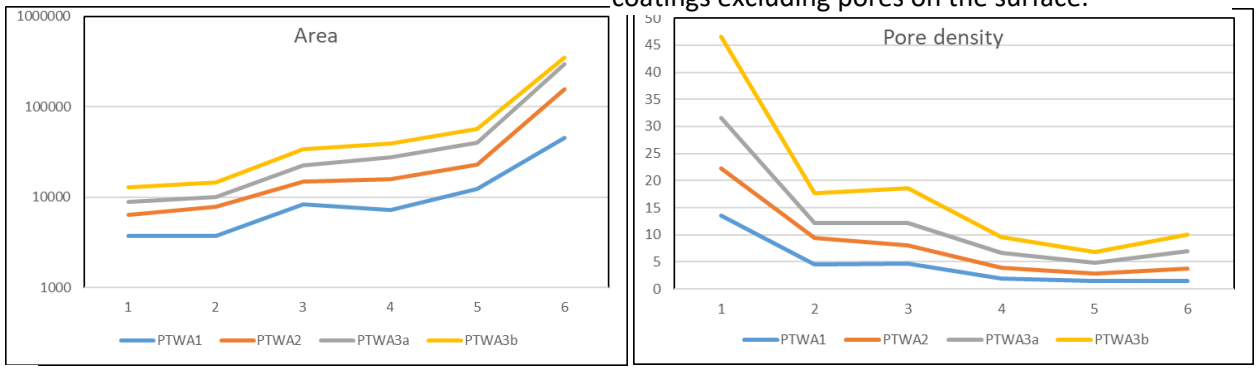

(a) (b)

Figure 28. (a) Pore size and (b) pore density distribution for PTWA coatings with different porosity levels.

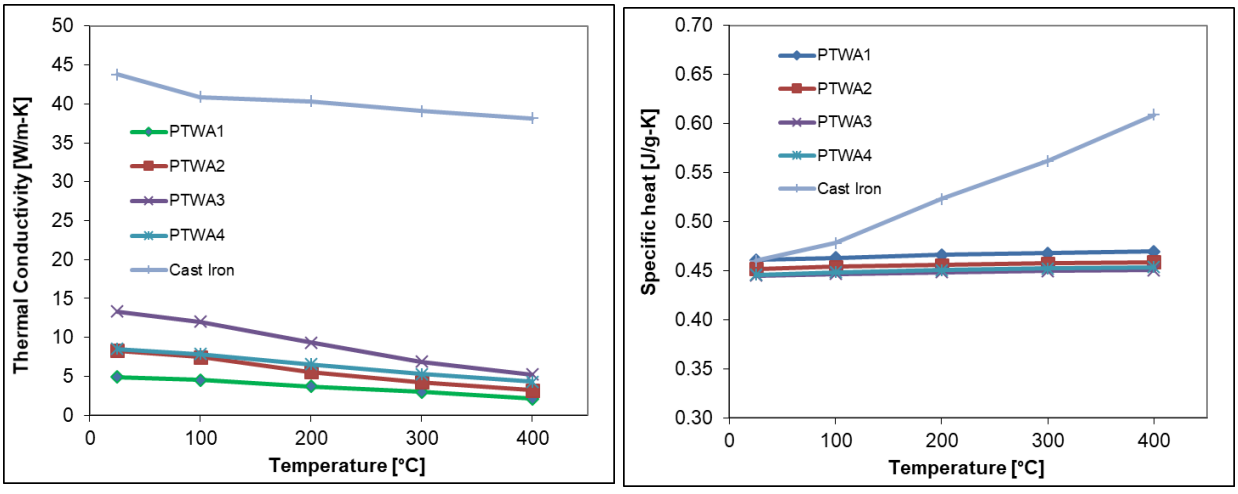

(a) (b)

Figure 29. A comparison of (a) thermal conductivity, and (b) specific heat of PTWA coatings and cast iron.

PTWA coatings remained unchanged with increasing temperature but the same for cast iron increased steadily.

3.2.2.4 Friction Measurements

Laboratory bench test (TE-77) -

Figure 30 shows coefficient of friction (as a function of (lubricant viscosity times velocity)) for PTWA coatings and compared with cast iron using a production top compression ring. The centerline average surface roughness (Ra) of the ring was 0.345 µm and that of the liner surface was 0.312 µm. The coefficient of friction of PTWA1 is found to be comparable of cast iron, which is not a surprise. As the porosity level in PTWA coatings increased (PTWA2 and PTWA3), friction benefit over cast iron could be observed in mixed lubrication regime (at higher values on x-axis) but in the boundary lubrication regime, the coefficient of friction is slightly higher than cast iron.

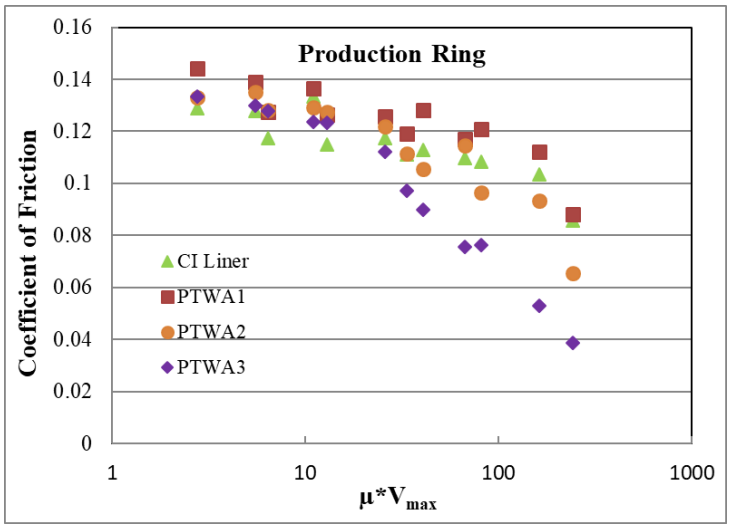

Figure 30. PTWA2 and PTWA3 showed friction benefits in mixed lubrication regime.

Figure 31 shows the effects of ring face coatings with high porosity PTWA3 coating. The surface roughness (Ra) of PVD (CrN) and DLC rings were 0.148 µm and 0.063 µm respectively. With production ring (Mo-NiCr coating) PTWA3 coated liner section showed a significant reduction of coefficient of friction in the mixed lubrication regime over cast iron.

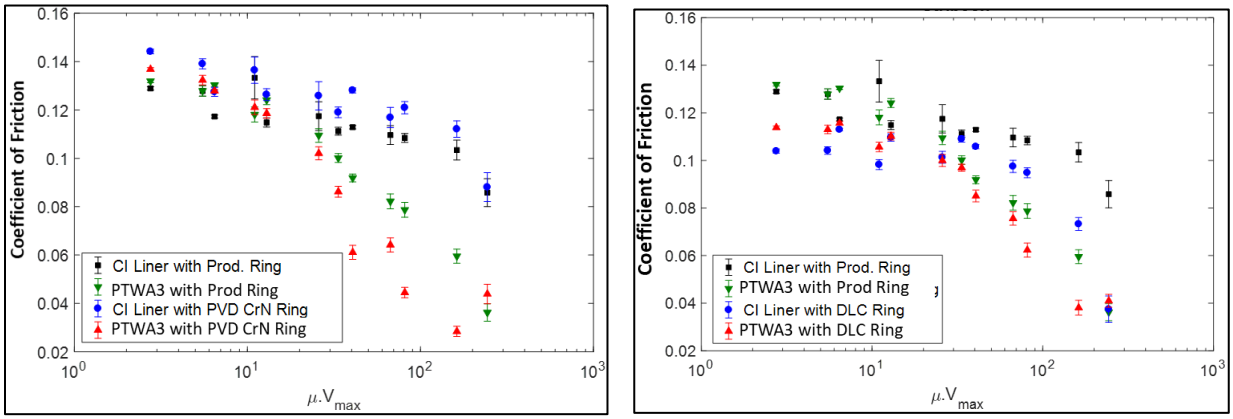

(a) (b)

Figure 31. The effect of ring face coatings on coefficient of friction with PTWA3 coating. (a) a comparison of production ring and PVD (CrN) coating, (b) a comparison of production ring and DLC coated ring.

The PVD ring performed similarly with cast iron as the production ring. However, with PTWA3 coating the PVD ring showed additional friction benefit over the production ring. In the boundary lubrication regime, no significant difference could be observed between cast iron liner and PTWA3 coating with either ring

coatings. Similar to PVD coated ring, the DLC coated ring also showed additional friction benefit over production ring with PTWA3 coating.

The friction reduction potential of nano-composite coatings was evaluated on ring-on-liner configuration at Argonne National Laboratory using the same procedure as described above. The results are shown in Figure 32. Both VN-NI and VN-Cu coatings showed significant reduction in coefficient of friction against PTWA3 coating in the mixed lubrication regime. However, the coefficient of friction values did not go as low as PVD CrN and DLC coatings (see Figure 31). But both coatings showed higher coefficient of friction in boundary lubrication regime over cast iron and production ring pair. VN-Cu coating did not offer any friction advantage over production Mo-NiCr coating against cast iron liner.

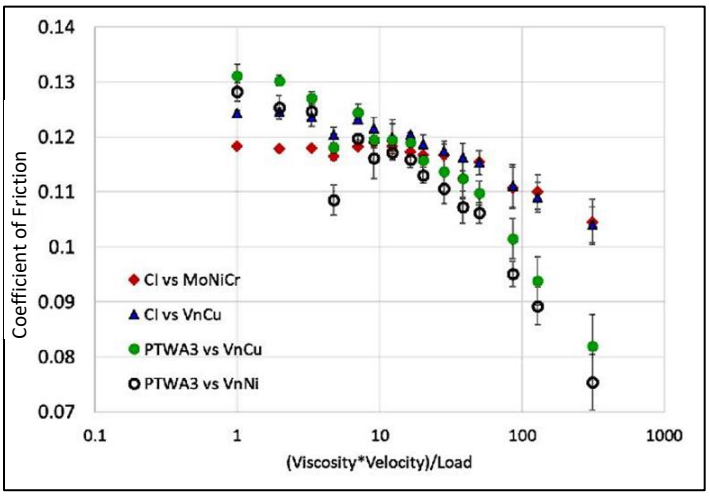

Figure 32. The effect of nano-composite coatings against cast iron and PTWA3 coating.

Motored Single Cylinder Friction – Figure 33 shows typical friction force traces at different temperatures with cast iron liner. Since there is no pressure acting on top of the piston, ring tension is the only load acting at the ring and liner interface. Each friction trace is the average of 100 traces. The positive friction

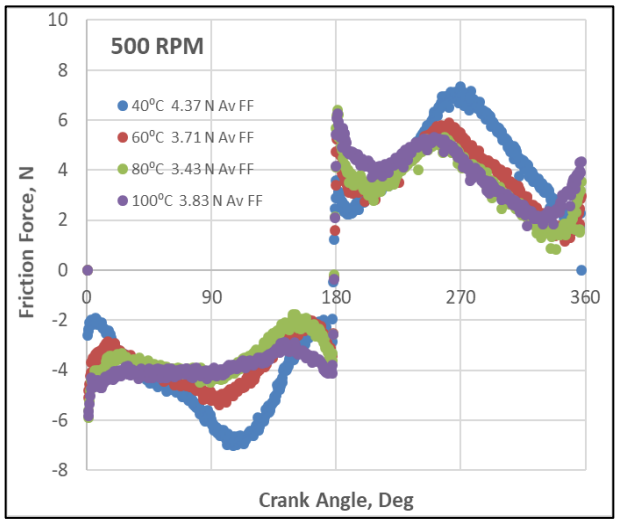

Figure 33. Friction force at piston liner interface as a function of crank angle at different

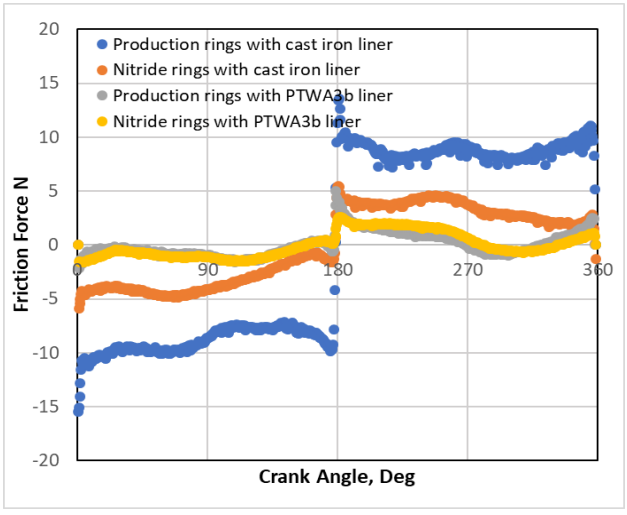

Figure 34. A comparison of friction force traces of PTWA3b coating and nitride piston rings over production liner and rings.

force values represent piston movement in one direction while the negative values represent piston movement in opposite direction. At zero degree crank angle, where the ring travel reverses, a high friction

force is recorded because of thin oil film thickness resulting in boundary lubrication condition. In the mid-stroke, where the piston velocity is highest, the oil film thickness is highest resulting in increase in friction force. The cycle average friction force values are also indicated in the legend. Generally, the average friction force deceased with increasing temperature. The increase in average friction force at 100°C is related to contributions from boundary and mixed lubrications. Figure 34 shows the effect of liner coating

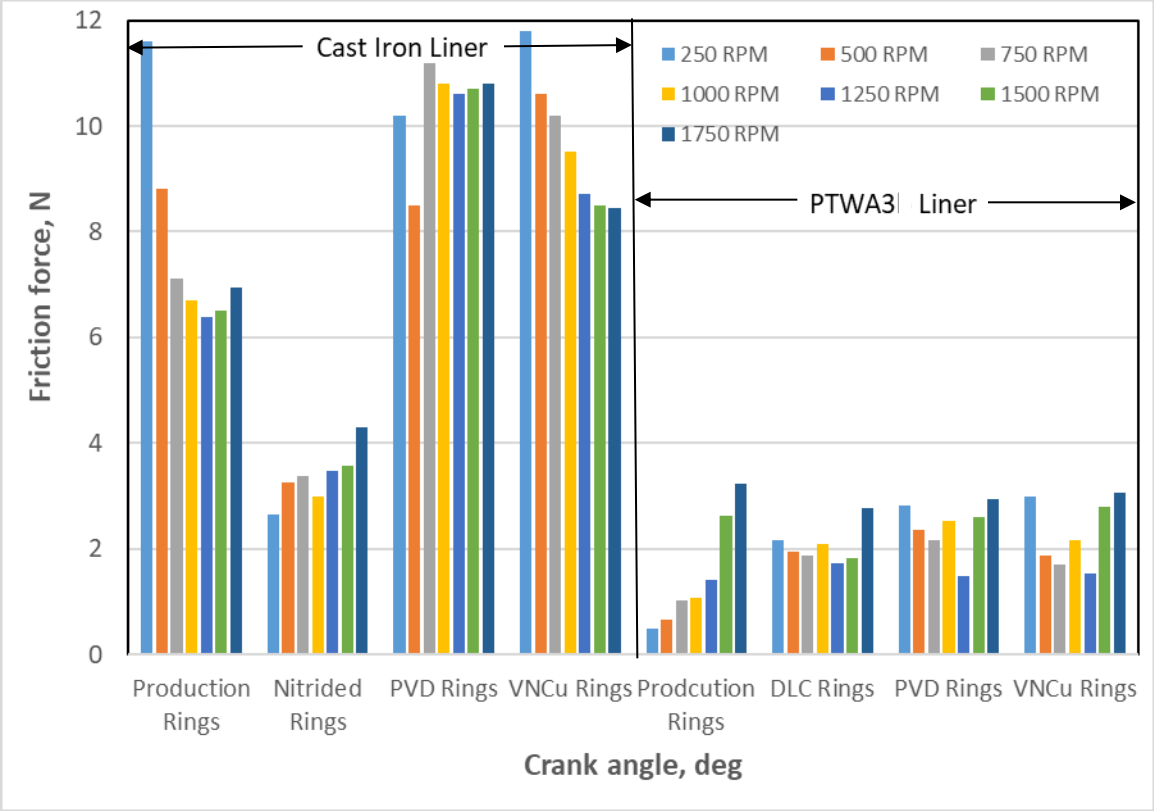

Figure 35. The average friction force measured for various ring face coatings against cast iron and PTWA3 coating.

(PTWA3) and ring coatings on friction force at 500 RPM and 100°C oil temperature. The nitrided piston ring pack includes top and oil control nitrided rings while a production second compression ring was used. The results show significant friction benefit with PTWA3 coating over production cast iron liner as demonstrated before. Also, nitride rings offer additional friction benefit with PTWA3 coating. Figure 35 summarizes all data at 100°C. In general, all rings in contact with PTWA3 coating showed lower friction force than cast iron liner and there was no significant differences between the ring coating technologies. The PVD rings showed lower friction force against cast iron liner at lower crankshaft speeds but the opposite was observed at higher speeds. A similar trend was observed with PTWA3 coating but the overall friction force was lower.

Motored Cranktrain Friction

(a) Cylinder bore and piston ring coatings

Figure 36 shows motored cranktrain friction results for PTWA coatings with different porosity levels and at different oil temperatures. The friction mean effective pressure (values derived from measured friction

torque) improvement over the production block (with production piston ring pack) is shown here. Therefore, values under one represent an improvement. At all temperatures, PTWA coatings showed a friction benefits over production block at all speeds with the exception of PTWA3a at 40°C oil temperature. The friction benefit increased with increased temperature and higher benefit is observed

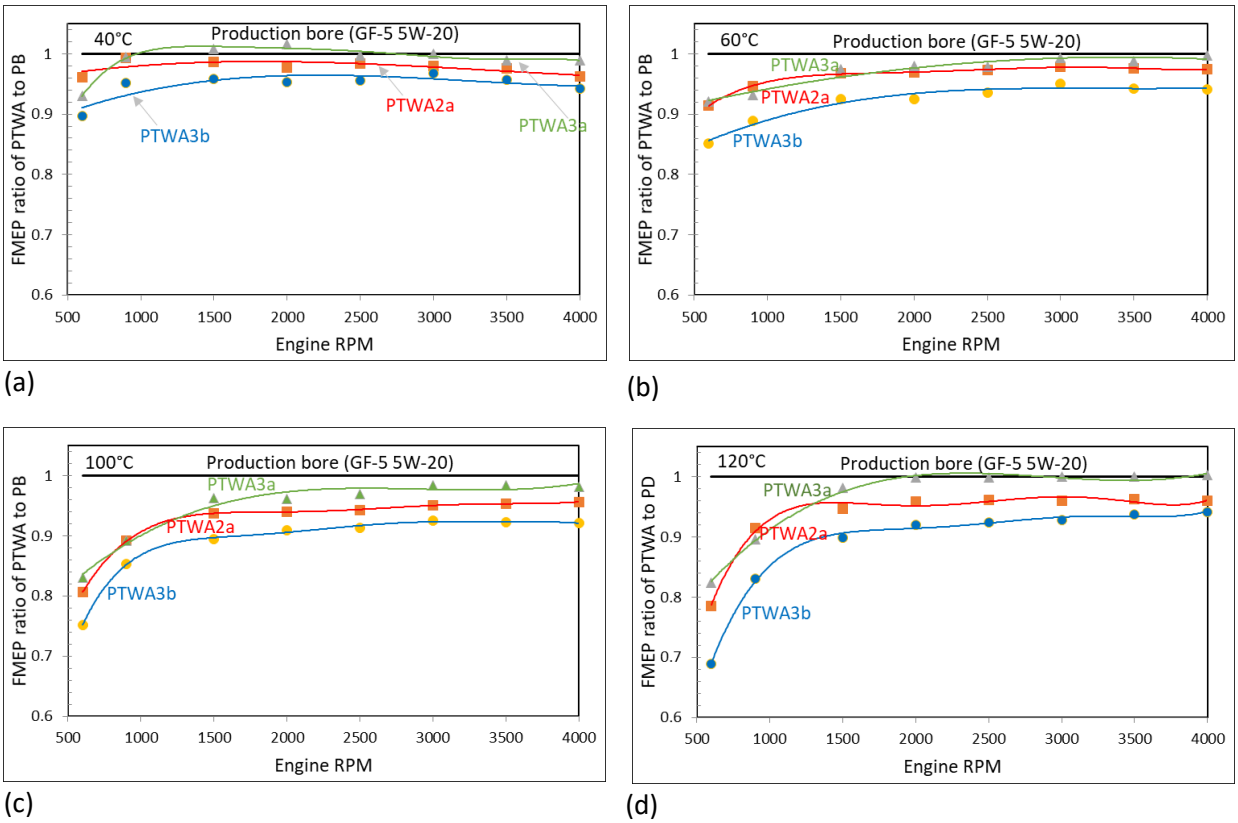

Figure 36. Friction benefits observed with PTWA coatings having different porosity levels at oil temperatures (a) 40°C, (b) 60°C, (c) 100°C, and (d) 120°C.

at lower speeds where mixed lubrication regime prevails. This result is consistent with laboratory bench test results where friction benefits were observed under mixed lubrication regime (shown in Figure 31). This is believed to be due to a combination of improved surface finish and presence of pores which act as oil reservoir facilitating hydrodynamic lift. Also, higher porosity level offered higher friction benefit with the exception of PTWA3a, the results of which is not clearly understood. Again, the general trend is in line with laboratory bench test results (shown in Figure 30).

The effect of ring face coatings on friction was evaluated with PTWA3b coating using the motored cranktrain friction rig. The average friction torque results with standard deviation are shown in Figure 37 for 120°C oil temperature. In general, the engine block with PTWA3b coating showed lower friction torque than the production block with cast iron liner block. At 1500 RPM, a reduction of 10 percent was observed. All rings (nitride, PVD CrN, and DLC) showed lower friction torque with PTWA3b coating than the production cast iron liner block with respective ring coatings. This is in line with laboratory bench test rig results. DLC coated rings with PTWA3b coating showed the lowest friction torque and at 1500 RPM a reduction of 22% is observed compared to production engine bock with production ring pack.

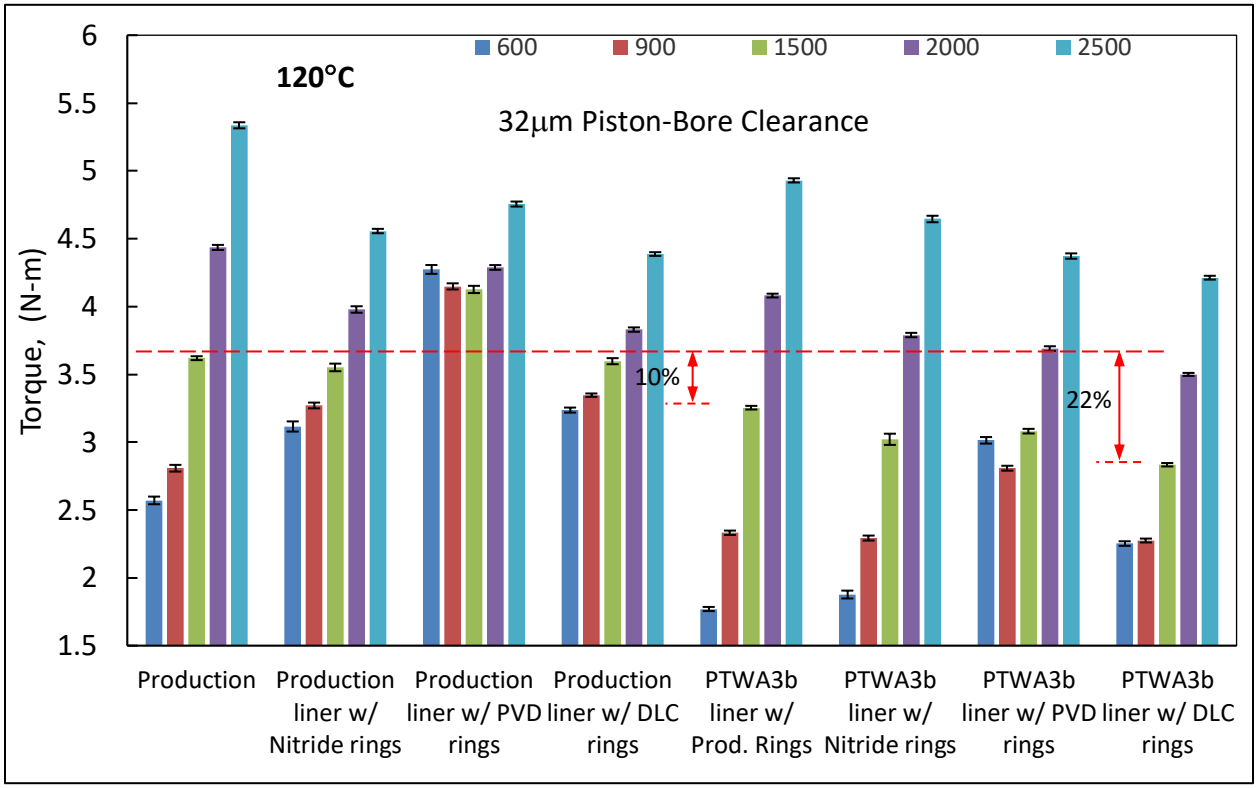

Figure 37. A comparison of motored cranktrain friction torque at 120°C oil temperature between various piston ring coatings with cast iron and PTWA3b coated blocks.

(b) Micro-polished Crankshaft

Table 5 shows enhancement of various surface roughness parameters by micro-polishing. It is to be noted that Main 2 and Main 3 journals were rougher than others prior to micro polishing but following micro-polishing the surface finish of journals were comparable.

Table 5. Surface roughness enhancement by micro-polishing

Roughness parameters (µm)	Main 1		Main 2		Main 3		Main 4		Main 5	
	Before	After	Before	After	Before	After	Before	After	Before	After
Ra	0.1582	0.06	0.416	0.05	0.3538	0.05	0.1157	0.06	0.0982	0.04
Rp	0.735	0.17	2.4406	0.16	1.5605	0.15	0.6869	0.17	0.3773	0.16
Rq	0.2212	0.08	0.7283	0.06	0.6591	0.07	0.162	0.09	0.1281	0.06
Rt	2.6761	0.85	11.3489	0.49	8.1749	0.72	1.5573	1.24	1.3613	0.74
Rv	0.6434	0.48	1.5892	0.27	1.154	0.36	0.4942	0.62	0.4201	0.37
Rz	1.3783	0.65	4.0298	0.42	2.7145	0.51	1.1811	0.79	0.7975	0.53
Rk	0.4483	0.16	0.9582	0.16	0.6736	0.14	0.3349	0.17	0.3161	0.13
Rpk	0.4324	0.05	1.7115	0.05	1.7755	0.04	0.2733	0.04	0.1141	0.04
Rvk	0.1848	0.16	0.9037	0.09	1.242	0.13	0.1638	0.18	0.1686	0.1
Mr1, (%)	11.26	7.497	13.71	8.13	10.88	8.241	13.09	7.129	8.95	8.671
Mr2, (%)	88.82	86.87	84.84	87.299	75.94	84.654	87.55	87.054	89.3	86.604

The friction results are shown in Figure 38 where friction torque is plotted as a function of engine RPM at 40°C, 60°C, 100°C, and 120°C for GF-5 SAE 5W-20 and PAG oils. Generally, micro-polished crankshaft showed a friction reduction with GF-5 SAE 5W-20 oil at higher speed, which is counter intuitive. The expectation was higher friction reduction at lower speeds, where lower oil film thickness is expected to have more asperity contacts and micro-polishing would reduce contact severity. The increased friction benefit at higher speeds may be related to slightly increased bearing clearance due to material removal by micro-polishing. The PAG oil showed a friction benefit over GF-5 SAE 5W-20 oil with production finish crankshaft at all speeds investigated probably due to its lower viscosity. The friction benefit at lower speeds can be explained by chemisorption of PAG molecules at the asperities (9).

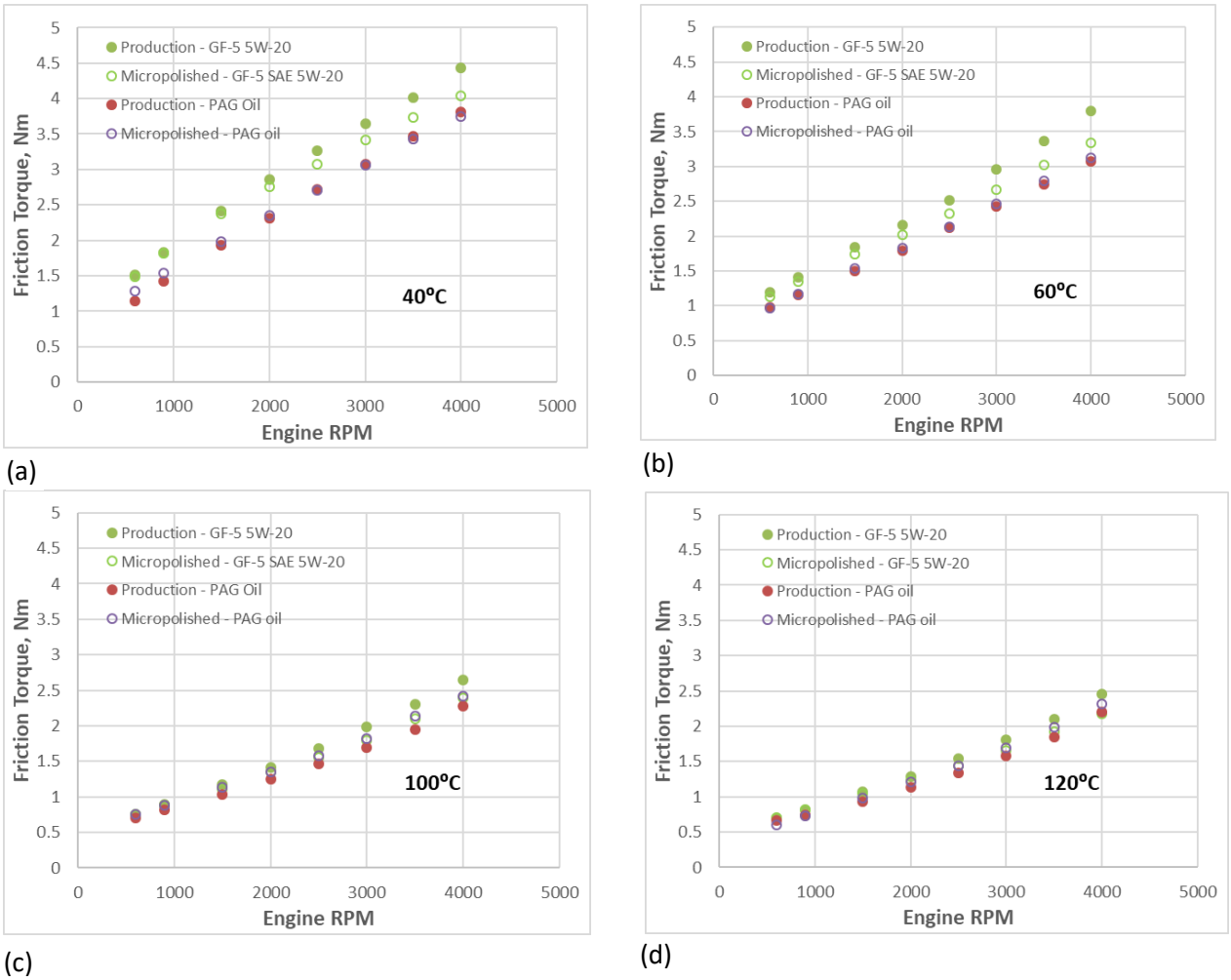

Figure 38. The effect of crankshaft micro-polishing on main bearing friction at (a) 40C, (b) 60C, (c) 100C, and (d) 120C.

Fired Single cylinder Friction – PTWA1 scuffed during the run-in portion of this program. Further investigation of the surface showed that the scuff initiated on the aluminum skirt of the piston. All pistons of this engine did not have any coating on the skirt area. It should be noted that all modern engine piston skirts have a solid lubricant based coating to prevent scuffing and NVH (noise vibration harshness) reduction. Figure 39 shows the friction results of PTWA coated liners and compared against uncoated

cast iron liner (CIL). Just over half (7/12) of the test points using the PTWA2 liner the frictional losses were lower than the cast iron liner –there are no data at three points for comparison and two where it is slightly higher. Some of the observations on the tests are as follows.

- For PTWA2 coating, there is no data at test points 11 and 12 as the engine would not produce the desired power. When measurements were processed, the friction was abnormally high showing that the piston assembly and liner scuffed during transition from test point 10 to 11. Figure 40 shows the end of test parts with the scuff marks on the thrust side. It is clear that the scuff was initiated at the aluminum skirt.
- For PTWA3 coating, it was not possible to get the engine to operate below 3.0Hp at test point 1, therefore this data point is invalid.
- For PTWA3 coating, it was not possible to get the engine to make the desired power at test point 12, therefore this data point is invalid. A scuff was suspected, but upon disassembly none was observed. Figure 41 shows end of test components. However, noticeable wear was observed on the piston skirt thrust side.

The results appear to indicate that mirror finished PTWA coated liners are not suited with uncoated pistons.

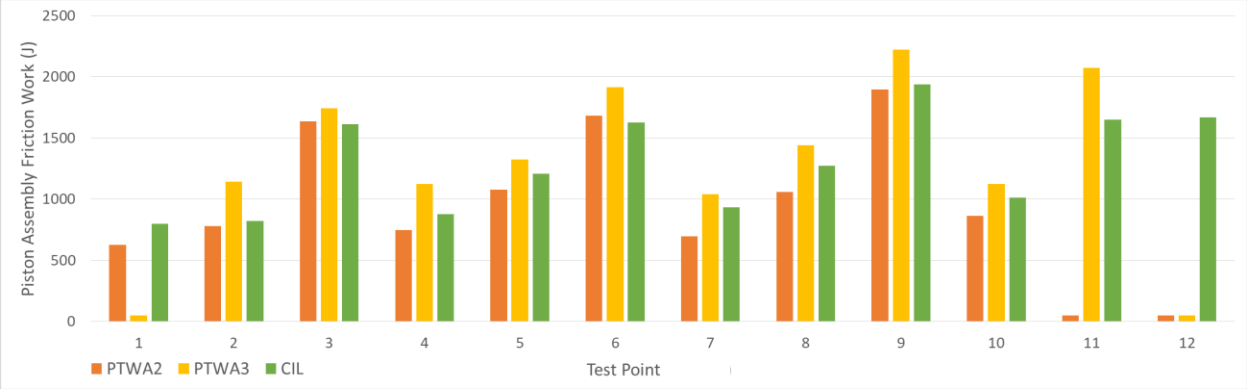

Figure 39. Fired single cylinder friction results on PTWA coated liners and compared to uncoated cast iron liner (CIL).

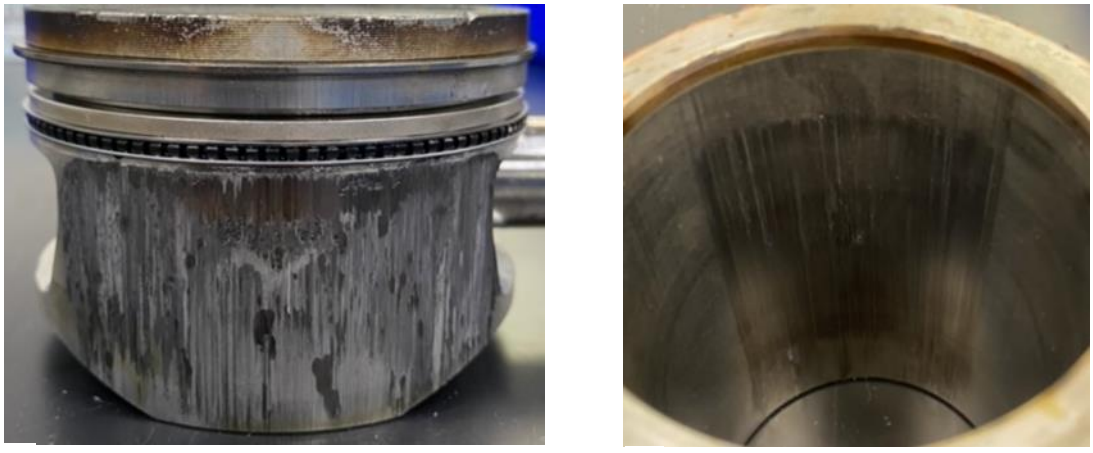

(a) (b)

Figure 40. Images of (a) piston skirt and (b) PTWA2 coated liner showing scuffing.

(a) (b)

Figure 41. Images of (a) piston skirt and (b) PTWA3 coated liner showing skirt scuffing.

Motored Engine Friction – The friction tests were performed as a function of engine speed. Each test was repeated five times and the average of all tests is reported. The standard deviation for each test point was calculated and it was smaller than the size of symbols. Figure 42 shows the friction results at 35^{o}C, 60^{o}C, 90^{o}C, and 120^{o}C oil temperatures. The friction data at 35^{o}C oil temperature is limited because of the inability of the test system to maintain a constant temperature. The general shape of the friction torque graphs point to engine operations in mixed and hydrodynamic lubrication regimes. Also, higher the temperature (lower the viscosity) lower the friction loss at a given speed level. The results in Figure 42 clearly shows the friction advantage offered by PTWA-coated blocks. Generally, higher the porosity level (the range investigated) higher the friction benefit observed with the exception of PTWA3a. At 90^{o}C

oil temperature, PTWA3b coated block with the highest porosity offered an average of 5% lower friction (averaged over the engine speed range) than the production block.

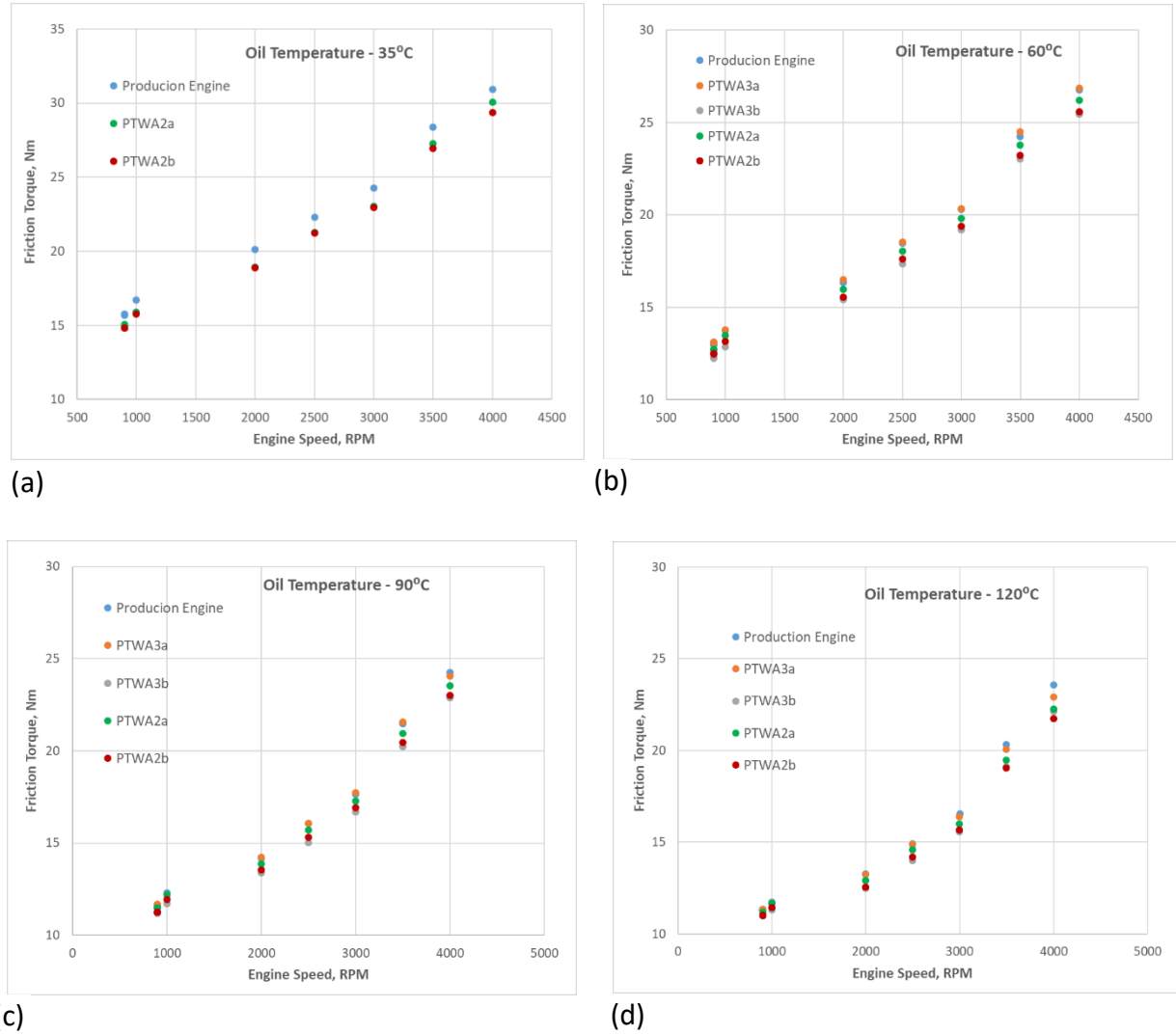

Figure 42. Motored engine friction torque as a function of engine speed at (a) 35°C, (b) 60°C, (c) 90°C, and (d) 120°C oil temperatures.

3.2.2.5 Cranktrain Wear Results

Cylinder bore wear as a function of time for different ring and bore material pairs is shown in Figure 43. Two general wear trends were seen. First, the wear rate was generally higher during the initial 20 hours as the ring-and-bore surfaces broke-in. Second, after the first 20 hours, the wear progressed fairly linearly with time. Our focus was on the steady-state wear rate of materials, which is more indicative of long term wear behavior. Repeatability with the baseline, cast iron bore and production rings, is shown in Figure 43a. The bore wear rate of the first test was 1.3 µg/hr, and 1.1 µg/hr for the repeat test. The higher level of noise in the repeat test was attributed to the lower activity level of the bore due to its decay with time. Cast iron and PTWA3 coated bore had a similar wear rate with current production rings and with PVD rings (Figure 43b). All combinations of bore and ring materials gave acceptable wear, but the lowest bore wear rate was seen with cast iron liners and DLC-coated rings (0.3 µg/hr) as shown in Figure 43c. Although PTWA3 wear rate was higher than cast iron with

DLC rings, it was comparable to cast iron liner-production ring pair. Higher initial wear was often seen with cast iron, compared to PTWA3 coated bore, which was attributed to the test sequence. The coated rings were new when they were installed in the engine block with cast iron liners, thus higher ring asperities were initially present. When the coated rings were re-used in the PTWA-coated engine block, the higher ring asperities were already worn away.

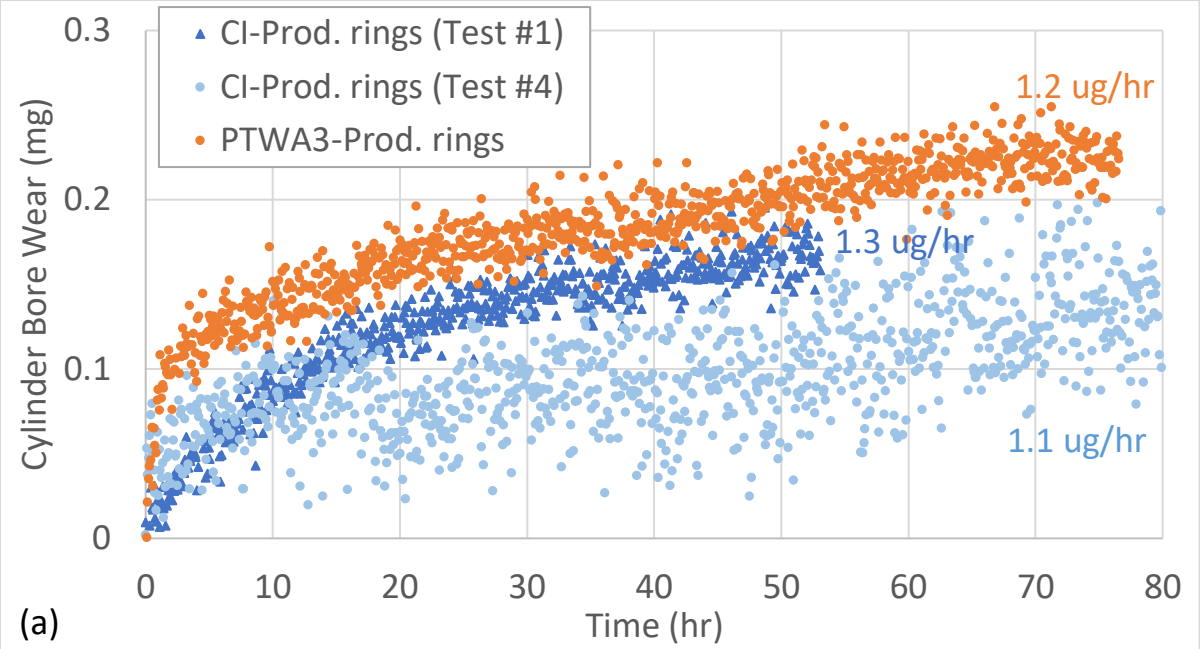

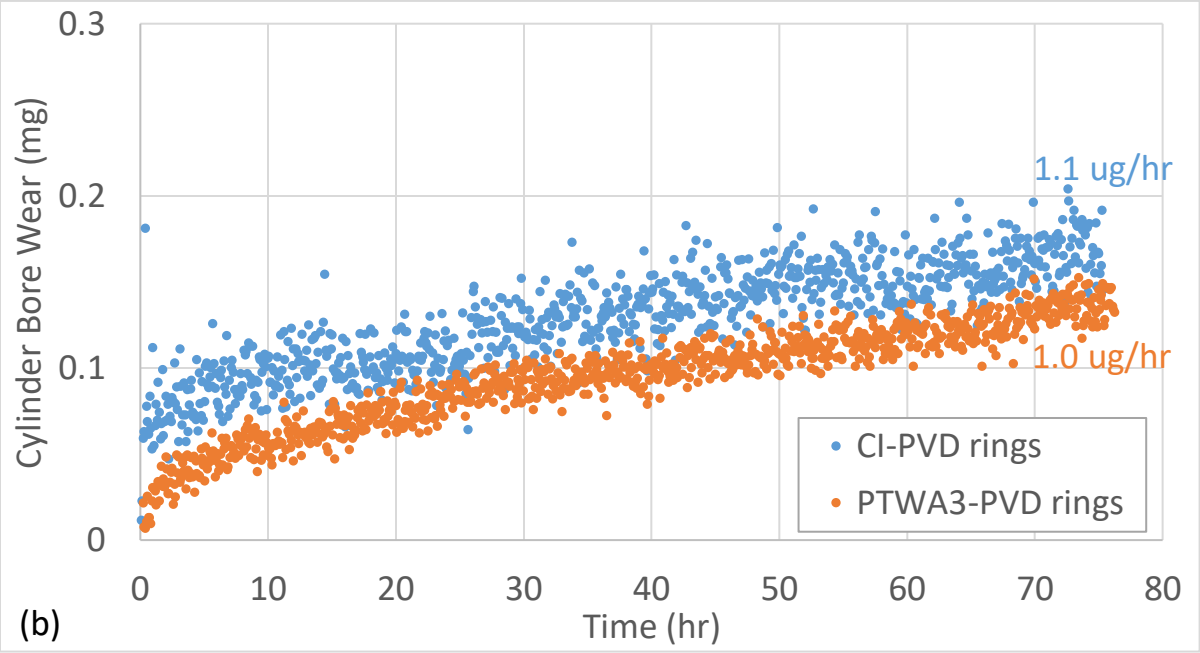

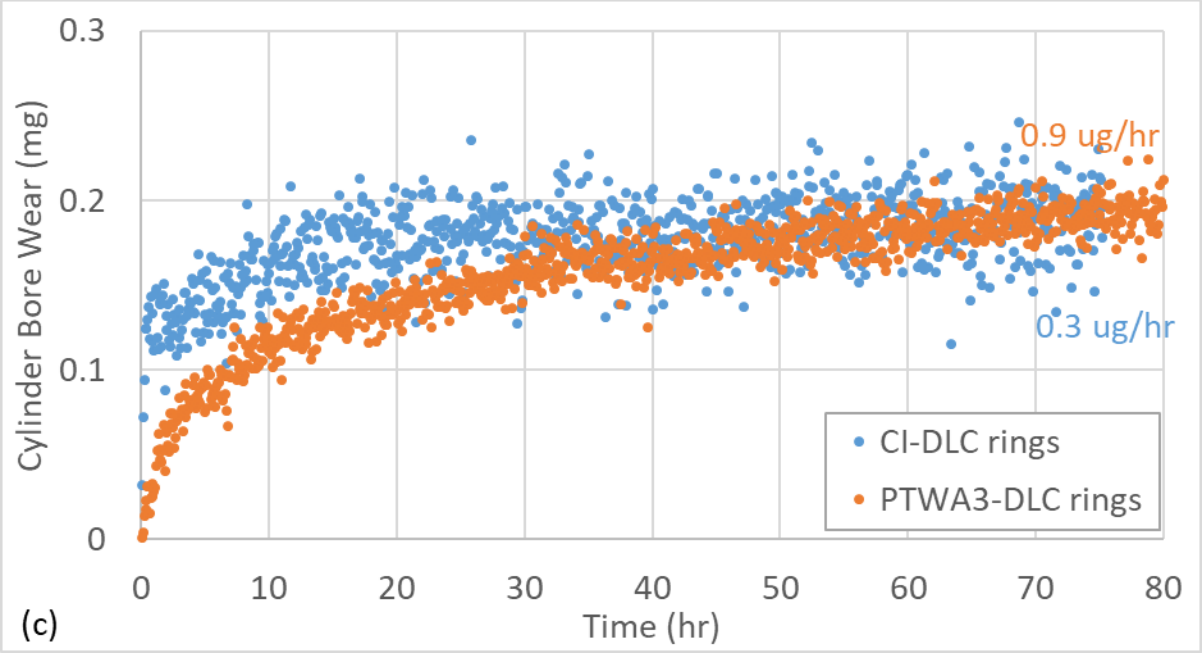

Figure 43. Comparison of cylinder bore wear with (a) current production, (b) CrN PVD, and (c) DLC-coated rings.

Oil control ring wear rate as a function of time for different ring and bore material pairs is shown in Figure 44. With steel nitrided rings, the wear rate was lower against cast iron liners (0.5 µg/hr) compared to PTWA3-coated bores (8.0 µg/hr). Similarly, with CrN PVD rings, the wear rate was lower against cast iron liners (0.1 µg/hr) compared to PTWA3-coated bores (15.0 µg/hr). With DLC-coated rings, the wear rate was low with either bore material. The combination of bore and ring wear rate of each material pair is summarized in Figure 45. The baseline pair of cast iron and nitrided steel rings showed a total of 1.5 µg/hr wear rate. The two material pairs with the lowest wear rate had DLC-coated rings.

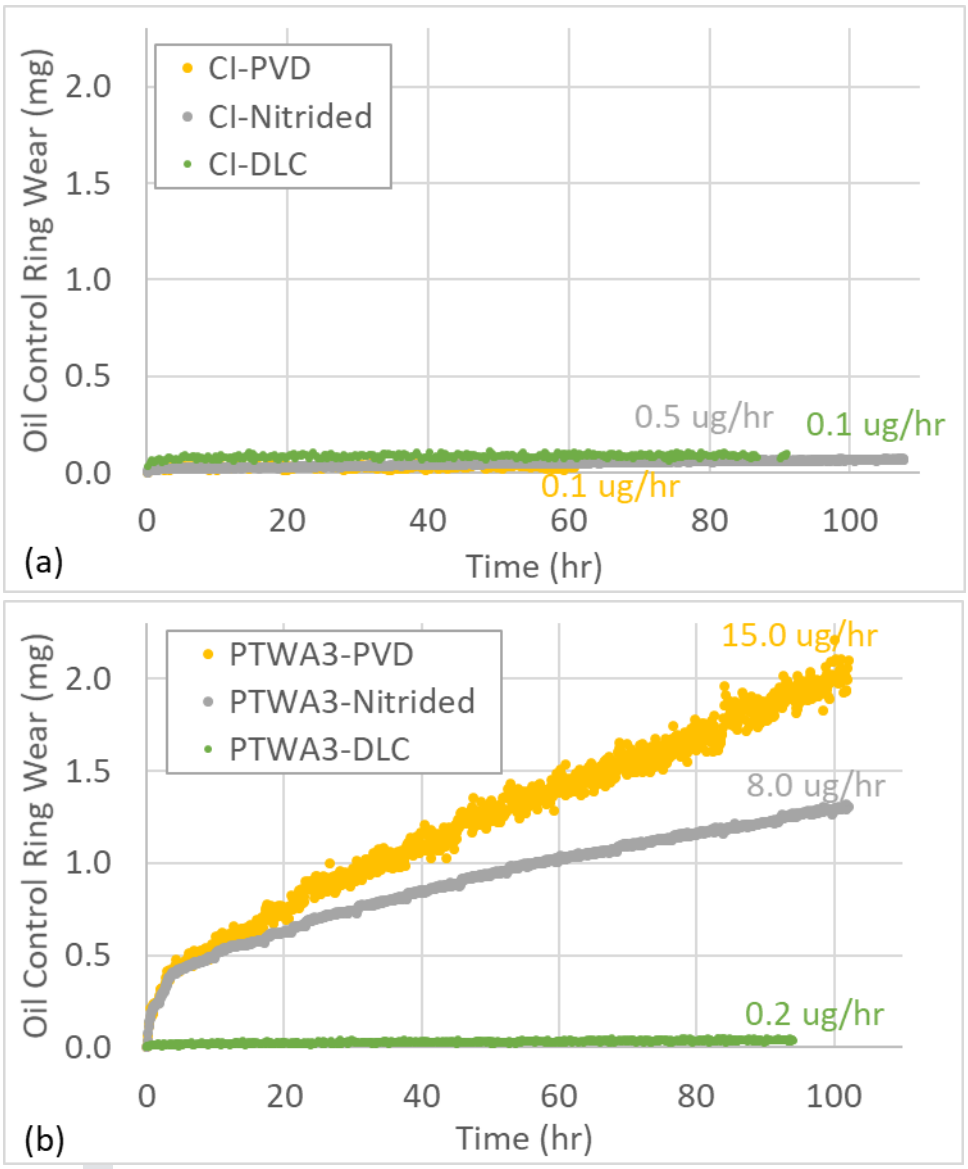

Figure 44. Comparison of oil control ring wear with (a) cast iron liners and (b) PTWA3-coated bores

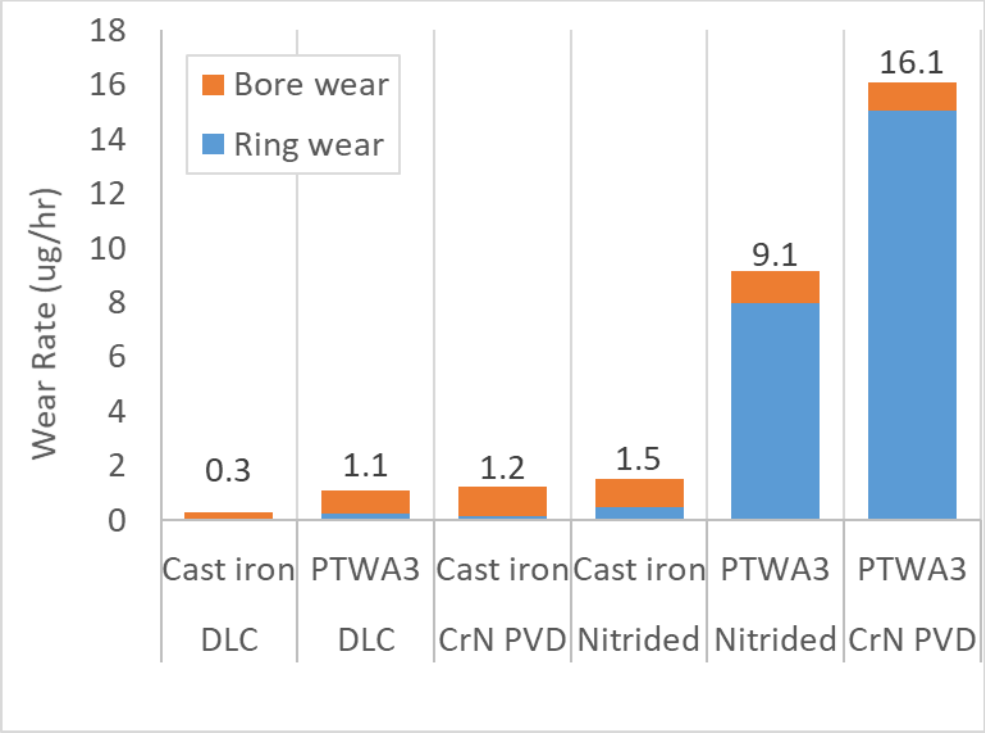

Figure 45. Ring and bore wear rate for all material pairs

3.2.2.6 Vehicle fuel economy

Chassis roll fuel economy tests were conducted on a sport utility vehicle with an inline four-cylinder engine. The results are shown Figure 46 in 95% confidence interval. The technology bundle with high porosity PTWA3b coating, DLC coated top and oil control rings (with production second compression ring) and polished crankshaft journals with GF-5 SAE 5W-20 oil showed no fuel economy benefit in city cycles but showed 3.11% and 0.76% benefit in highway and combined metro-highway cycles respectively. With PAG oil, fuel economy benefits of 4.15%, 5.71%, and 4.7% in city, highway and combined metro-highway cycles respectively were observed. The significantly higher benefit with PAG oil can be explained in part by its lower viscosity, and the chemistry of the base oil. It has been observed in the past DOE project (8,9) that PAG oil being polar in nature reduce friction significantly by adsorption of polar molecules on sliding/rolling surfaces. It is possible there could be synergistic effect between PAG oil chemistry and PTWA3b and DLC coatings improving fuel economy benefit. There were not enough time and resources available to investigate this effect. Also, there could be variation in fuel economy numbers due to engine block exchanges for which there is no statistical data available.

Although PAG oil showed significant fuel economy benefit, it should be noted that there are durability issues related to wear, and varnish formation, and high temperature oxidation performance. These issues are related to limited choice of additive components that are compatible with this base oil.

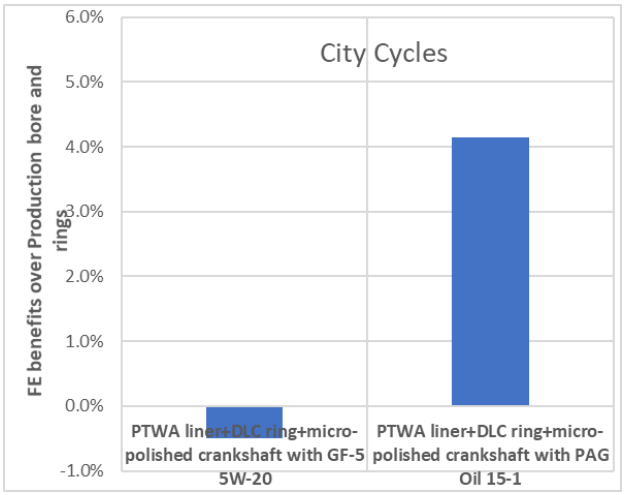

(a)

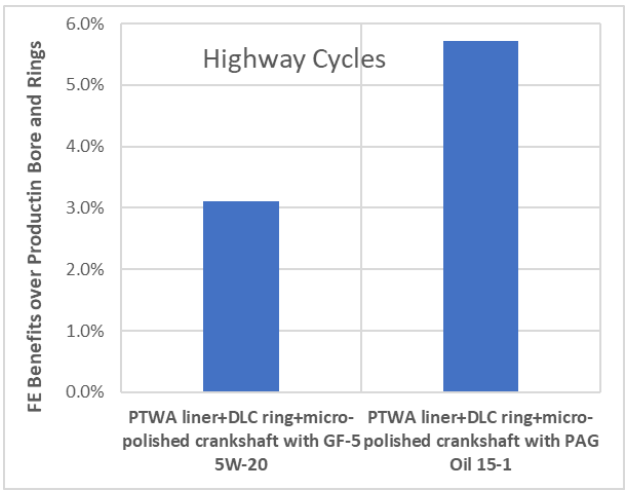

(b)

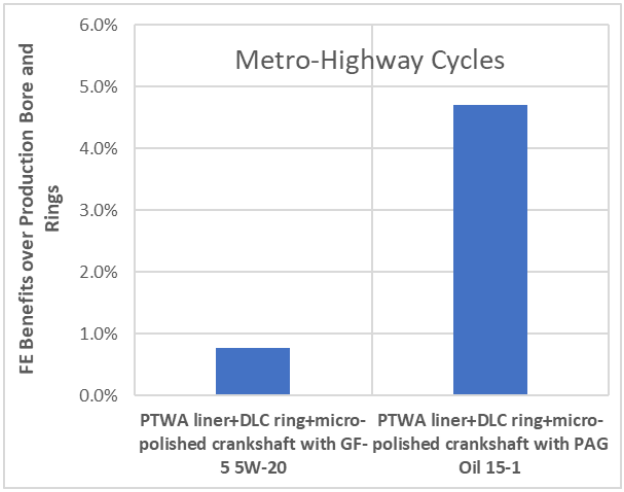

(c)

Figure 46. Chassis roll fuel economy benefits of technology bundle over current production engine with GF-5 SAE 5W-20 and PAG oil 15-1 oils under (a) city cycles, (b) highway cycles, and (c) combined metro-highway cycles.

4. Conclusions

Some of the key conclusions from this investigation are as follows

a. The investigation identified key PTWA coating deposition parameters and their levels for generating high porosity levels (2-16%). These parameters include atomizing gas pressure, plasma gas flow rate, plasma current, and wire feed rate for a given plasma torch design.

b. The investigation also identified key cylinder bore honing conditions for generating additional porosity and desired surface finish for friction reduction. The mechanisms of porosity generation are also identified which includes, delamination of thin surface layers and removal of not-fully molten particles during honing, and naturally occurring pores during coating deposition.

c. Established various methods for characterizing pores; the size, area density, and size distribution using optical microscopy (2D and 3D), and laser interferometry technique (3D).

d. Laboratory bench friction tests showed friction reduction with high porosity PTWA coating compared to cast iron liner under mixed lubrication regime. The friction benefit increased with increasing porosity level. The friction reduction further increased with the choice of ring face coating; DLC coated ring showed the lowest friction.
e. Motored cranktrain and single cylinder friction tests showed similar results as the laboratory bench tests. Motored friction tests on an inline four cylinder engine showed 0.8Nm (5.4%) reduction in friction torque at 90^{o}C and 2000 engine rpm with PTWA3 coated block in comparison to a production engine with cast iron liner.
f. Single cylinder fired engine friction tests generally showed a friction reduction but also showed evidence of scuffing on piston skirt and liner surfaces indicating pistons without a skirt coating is not well suited for high porosity mirror finished PTWA coating.
g. The wear rate of PTWA3 coating was comparable to cast iron liner with production and PVD rings. However, DLC rings are best suited with PTWA3 coating because of comparable PTWA3 wear rate with cast iron liner, and significantly lower ring wear rate and reduced friction.
h. A combination of PTWA3 coated cylinder block, DLC top and oil control rings, and micro-polished crank journals on an inline 4 cylinder engine showed 0.8% fuel economy benefit over production engine in metro-highway cycles with GF-5 SAE 5W-20 oil. However, with PAG oil, the fuel economy benefit was 4.7% in metro-highway cycles partly because of its lower viscosity and the chemistry of the base oil.

References

1. O. Pinkus, and D.F. Wilcock, “Strategy for energy conservation through tribology”, New York, ASME, 1977.
2. T.E. Kiovsky, N.C. Yates, and J.R. Bales, “Fuel efficient lubricants and the effect of base oils”, Lubrication Engineering, April 1994.
3. K. Funatani, I. Kurusawa, A. Fabiyi, and M.F. Puz, "Engine performance improvements", Automotive Engineering, I, p15-20, 1995.
4. L. Shi, C.F. Sun, F. Zhou, and W.M. Liu, "Electrodeposited nickel-cobalt composite coating containing nano-sized Si3N4", Materials Science and Engineering A, 397, pp190-194, 2005.
5. V.D.N Rao, D.M. Kabat, R. Rose, D. Yeager, R. Brandt, and D.Y. Leong, “Performance of plasma spray coated bore 4.6L –V8 aluminum block engines in dynamometer and fleet vehicle durability tests”, Society of Automotive Engineers Paper No. 980008, SAE International.
6. B. Pope, “Ford Shelby GT500 Mustang Loses Weight, Gains Power”, WardsAuto.com, Feb 9, 2010.
7. F. Steinparzer, H. Unger, T. Brüner, D. Kannenberg, “The new BMW 2.0 litre 4-cylinder S.I. engine with Twin Power Turbo Technology”, Internationales Wiener Motorensymposium, 2011.
8. “Development of Modified PAG (Polyalkylene Glycol) High VI High Fuel Efficient Lubricant for LDV Applications”, Final Technical Report U.S. Department of Energy Award DE-EE0005388, December 2015.

9. A. Gangopadhyay, A., McWatt, D.G., Zdrodowskia, R.J., Simko, S.J., Peczonczyk, S.L., Cuthbert, J., Hock, E.D.,"Valvetrain Friction and Wear Performance of Polyalkylene Glycol Engine Oils", Tribology Transactions (2018), Vol. 61, pp133-143.